Atomistic simulation study on the silicon carbide precipitation in silicon

F. Zirkelbach

Yet another seminar talk

Augsburg, 26. Mai 2011

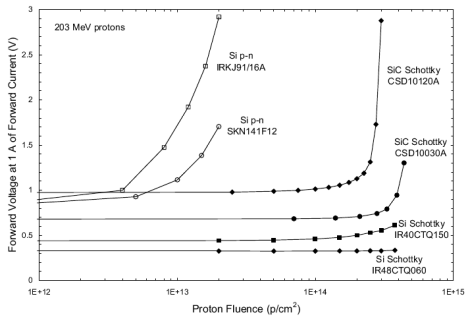

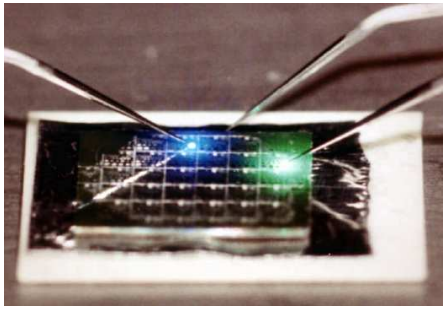

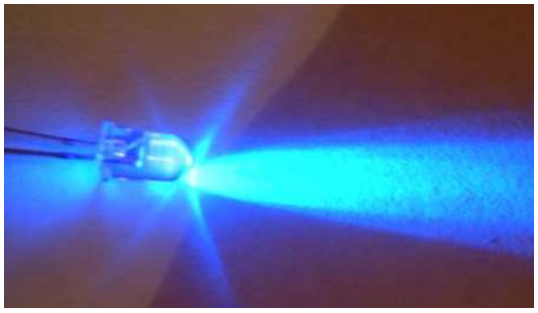

PROPERTIES

wide band gap

high electric breakdown field

good electron mobility

high electron saturation drift velocity

high thermal conductivity

hard and mechanically stable

chemically inert

radiation hardness

APPLICATIONS

high-temperature, high power
and high-frequency
electronic and optoelectronic devices

material suitable for extreme conditions
microelectromechanical systems
abrasives, cutting tools, heating elements

first wall reactor material, detectors
and electronic devices for space

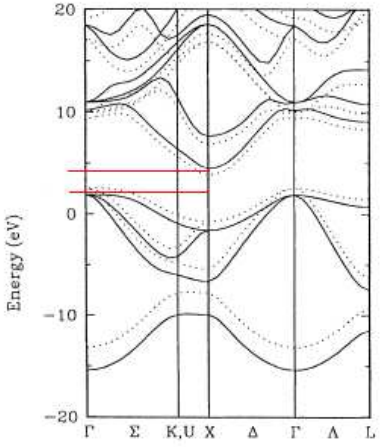

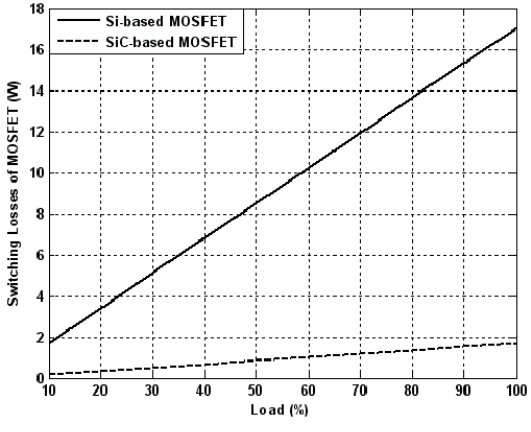

Polytypes of SiC

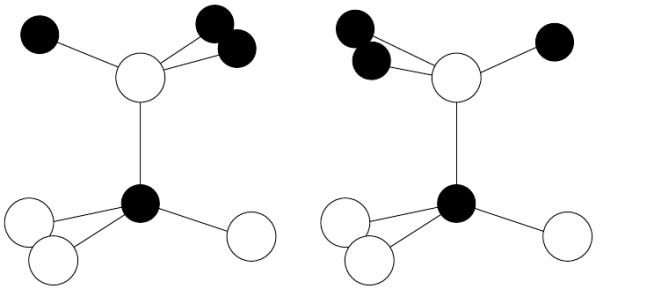

cubic (twist) hexagonal (no twist)

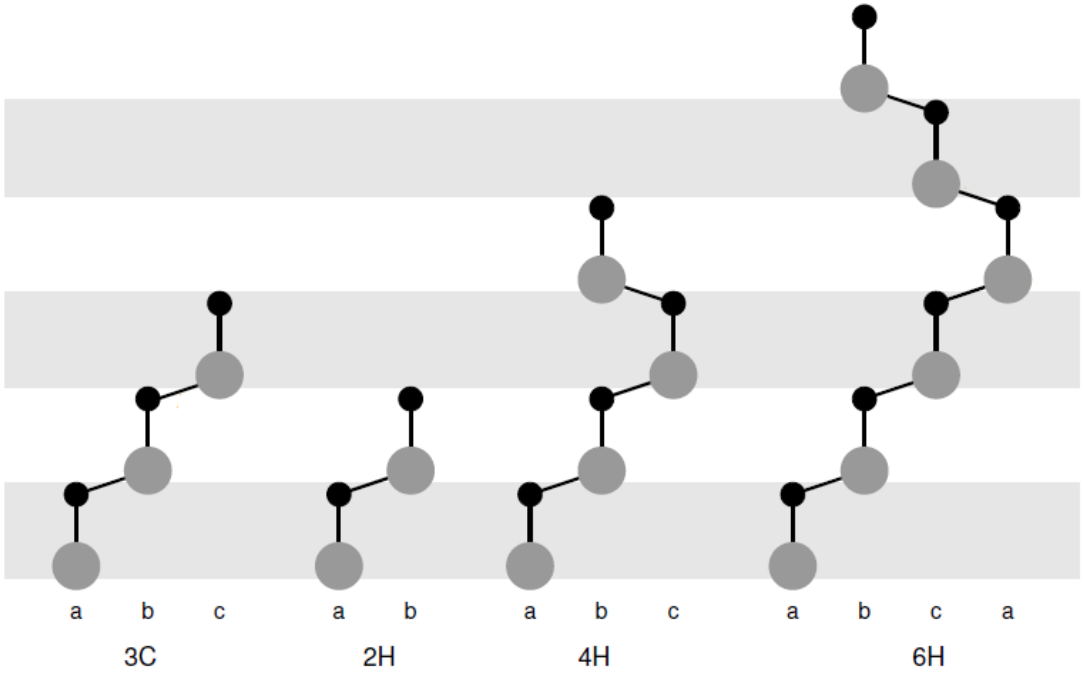

	3C-SiC	4H-SiC	6H-SiC	Si	GaN	Diamond
Hardness [Mohs]		—— 9.6 ——		6.5	-	10
Band gap [eV]	2.36	3.23	3.03	1.12	3.39	5.5
Break down field [10^6 V/cm]	4	3	3.2	0.6	5	10
Saturation drift velocity [10^7 cm/s]	2.5	2.0	2.0	1	2.7	2.7
Electron mobility [cm^2/Vs]	800	900	400	1100	900	2200
Hole mobility [cm^2/Vs]	320	120	90	420	150	1600
Thermal conductivity [W/cmK]	5.0	4.9	4.9	1.5	1.3	22

Values for $T = 300$ K

Fabrication of silicon carbide

SiC - *Born from the stars, perfected on earth.*

Conventional thin film SiC growth:

- Sublimation growth using the modified Lely method
  - SiC single-crystalline seed at $T = 1800\,^{\circ}\mathrm{C}$
  - Surrounded by polycrystalline SiC in a graphite crucible at $T = 2100 - 2400\,^{\circ}\mathrm{C}$
  - Deposition of supersaturated vapor on cooler seed crystal
- Homoepitaxial growth using CVD
  - Step-controlled epitaxy on off-oriented 6H-SiC substrates
  - $C_3H_8/SiH_4/H_2$ at $1100 - 1500\,^{\circ}\mathrm{C}$
  - Angle, temperature $\rightarrow$ 3C/6H/4H-SiC
- Heteroepitaxial growth of 3C-SiC on Si using CVD/MBE
  - Two steps: carbonization and growth
  - $T = 650 - 1050\,^{\circ}\mathrm{C}$
  - SiC/Si lattice mismatch $\approx 20\,\%$
  - Quality and size not yet sufficient

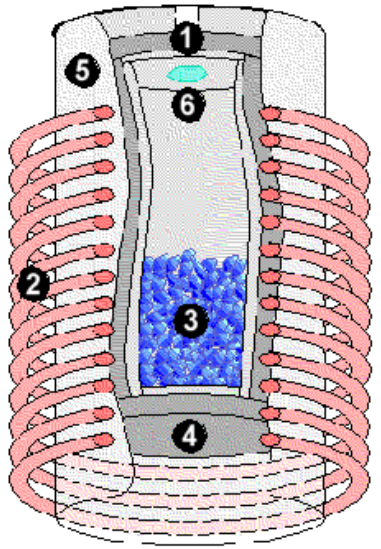

1. Lid
2. Heating
3. Source
4. Crucible
5. Insulation
6. Seed crystal

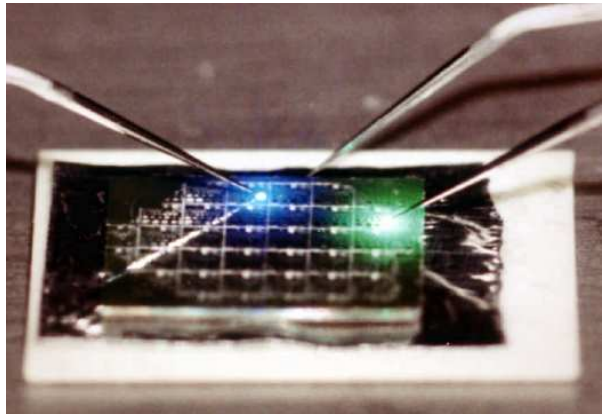

NASA: 6H-SiC and 3C-SiC LED on 6H-SiC substrate

Hex: micropipes along c-axis

3C-SiC fabrication less advanced

Fabrication of silicon carbide

Alternative approach: Ion beam synthesis (IBS) of burried 3C-SiC layers in Si(1 0 0)

- Implantation step 1
  180 keV C^+, $D = 7.9 \times 10^{17}$ cm^{-2}, $T_i = 500\,^\circ$C
  $\Rightarrow$ box-like distribution of equally sized and epitactically oriented SiC precipitates
- Implantation step 2
  180 keV C^+, $D = 0.6 \times 10^{17}$ cm^{-2}, $T_i = 250\,^\circ$C
  $\Rightarrow$ destruction of SiC nanocrystals in growing amorphous interface layers
- Annealing
  $T = 1250\,^\circ$C, $t = 10$ h
  $\Rightarrow$ homogeneous, stoichiometric SiC layer with sharp interfaces

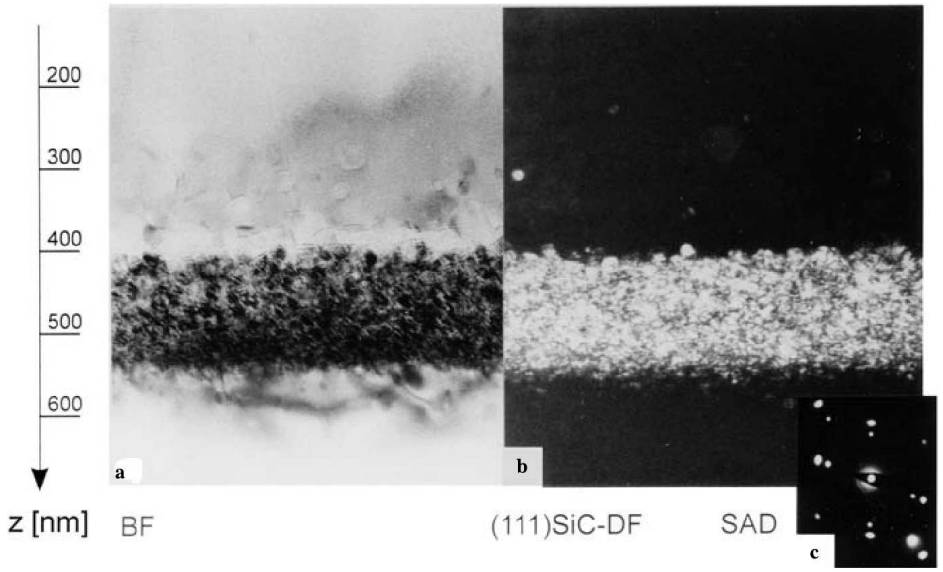

XTEM micrograph of single crystalline 3C-SiC in Si(1 0 0)

Precipitation mechanism not yet fully understood!

Understanding the SiC precipitation

$\Rightarrow$ significant technological progress in SiC thin film formation

$\Rightarrow$ perspectives for processes relying upon prevention of SiC precipitation

Outline

- Supposed precipitation mechanism of SiC in Si
- Utilized simulation techniques
  - Molecular dynamics (MD) simulations
  - Density functional theory (DFT) calculations
- C and Si self-interstitial point defects in silicon
- Silicon carbide precipitation simulations
- Summary / Conclusion / Outlook

Supposed precipitation mechanism of SiC in Si

Si & SiC lattice structure

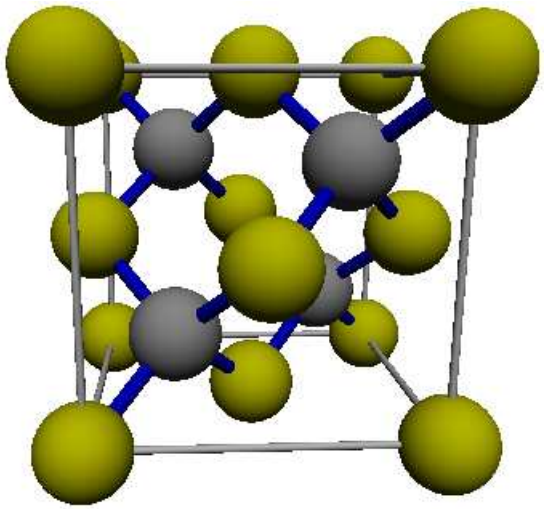

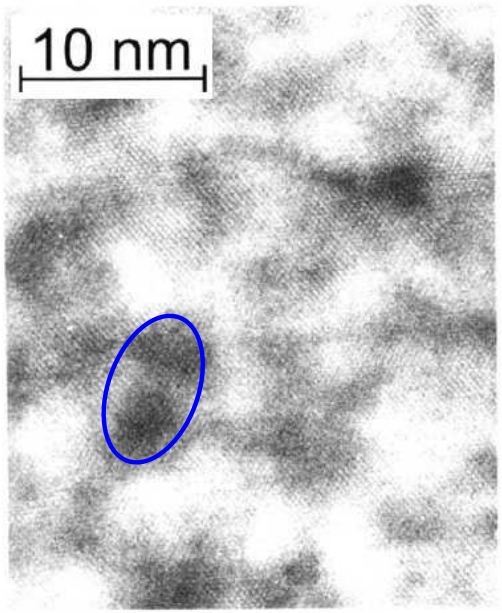

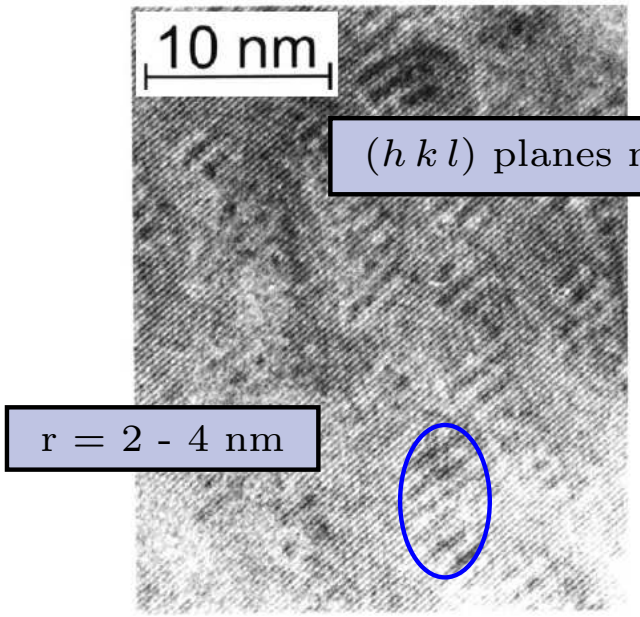

C-Si dimers (dumbbells)
on Si interstitial sites

Agglomeration of C-Si dumbbells
⇒ dark contrasts

Precipitation of 3C-SiC in Si
⇒ Moiré fringes
& release of Si self-interstitials

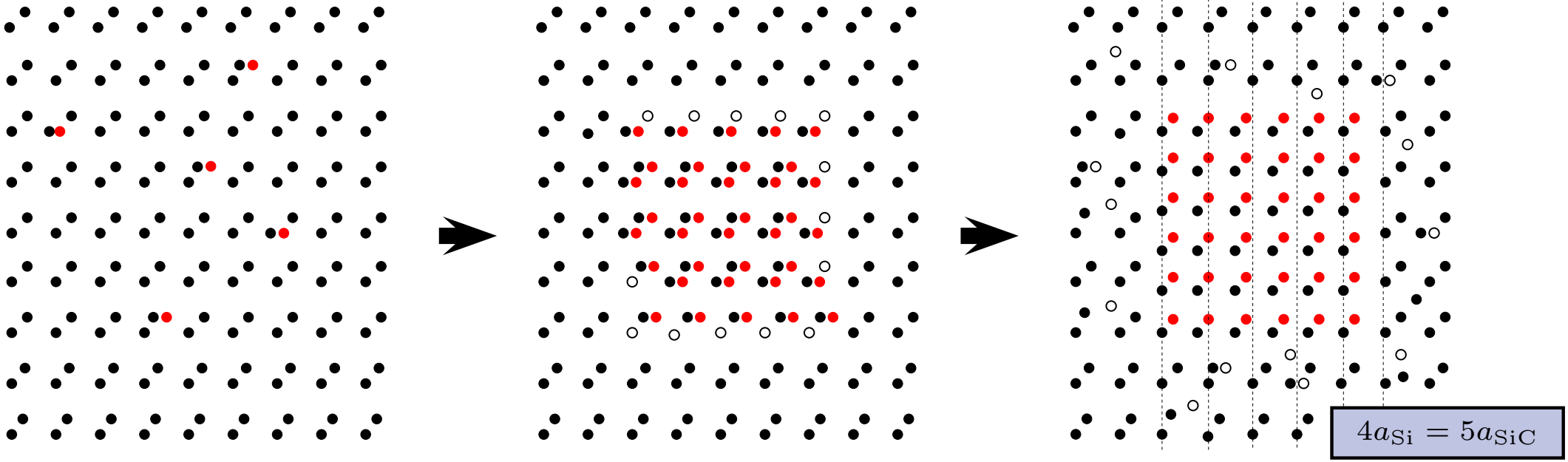

Supposed precipitation mechanism of SiC in Si

Si & SiC lattice structure

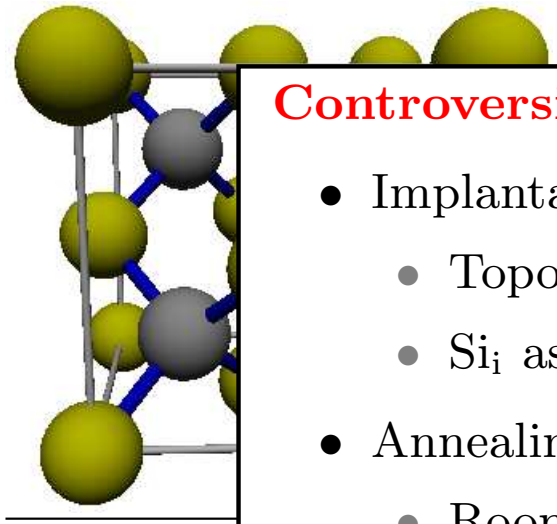

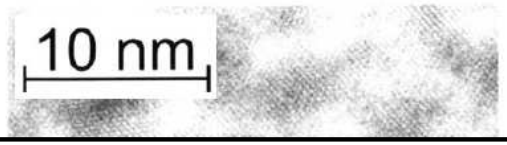

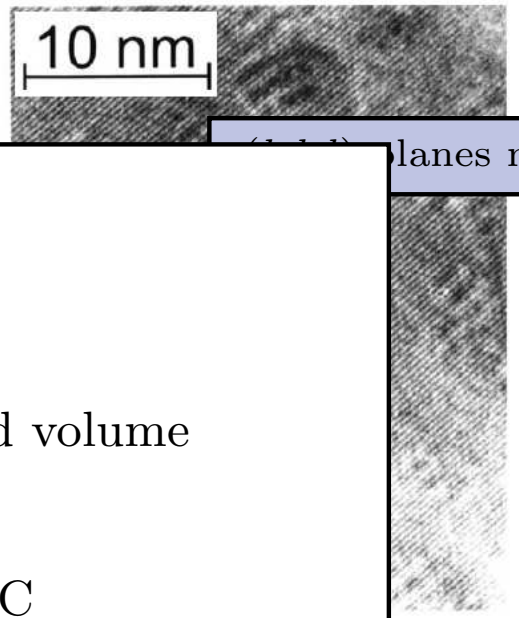

lanes match

C in Si

rstitials

C-Si din
on Si i

Controversial views

- Implantations at high T (Nejim et al.)
  - Topotactic transformation based on C_{sub}
  - Si_i as supply reacting with further C in cleared volume
- Annealing behavior (Serre et al.)
  - Room temperature implants → highly mobile C
  - Elevated T implants → no/low C redistribution/migration (indicate stable C_{sub} configurations)
- Strained silicon & Si/SiC heterostructures
  - Coherent SiC precipitates (tensile strain)
  - Incoherent SiC (strain relaxation)

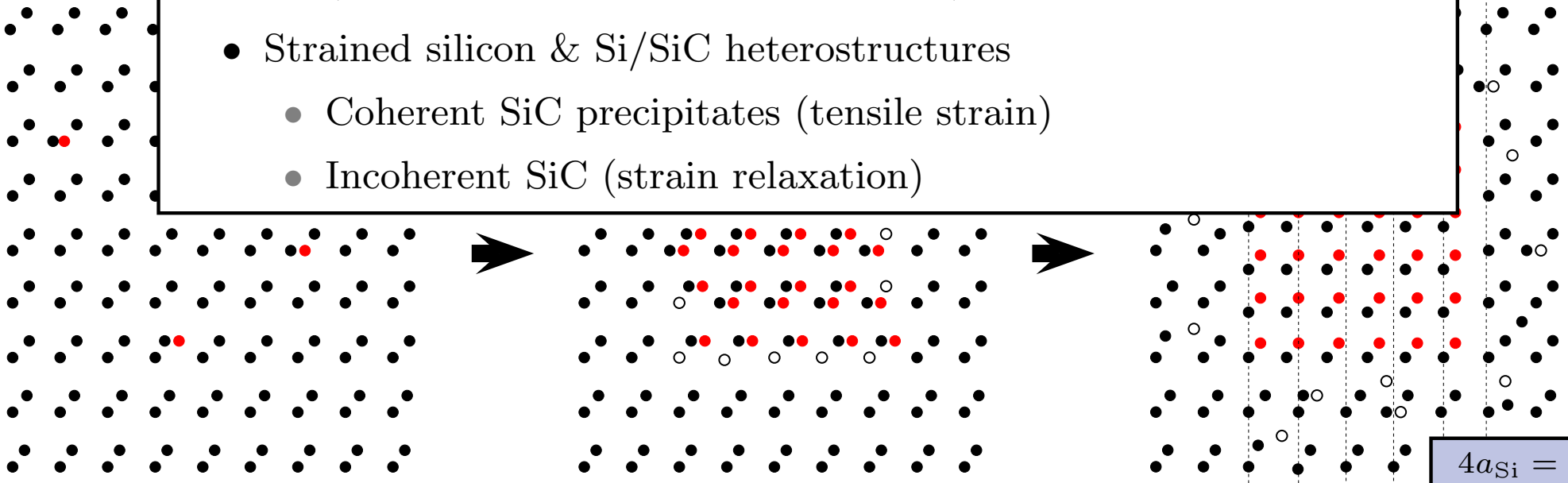

$4a_{Si} = 5a_{SiC}$

Molecular dynamics (MD) simulations

MD basics:

- Microscopic description of N particle system
- Analytical interaction potential
- Numerical integration using Newtons equation of motion as a propagation rule in 6N-dimensional phase space
- Observables obtained by time and/or ensemble averages

Details of the simulation:

- Integration: Velocity Verlet, timestep: 1 fs
- Ensemble: NpT (isothermal-isobaric)
  - Berendsen thermostat: $\tau_\mathrm{T} = 100$ fs
  - Berendsen barostat:
    $\tau_\mathrm{P} = 100$ fs, $\beta^{-1} = 100$ GPa
- Erhart/Albe potential: Tersoff-like bond order potential

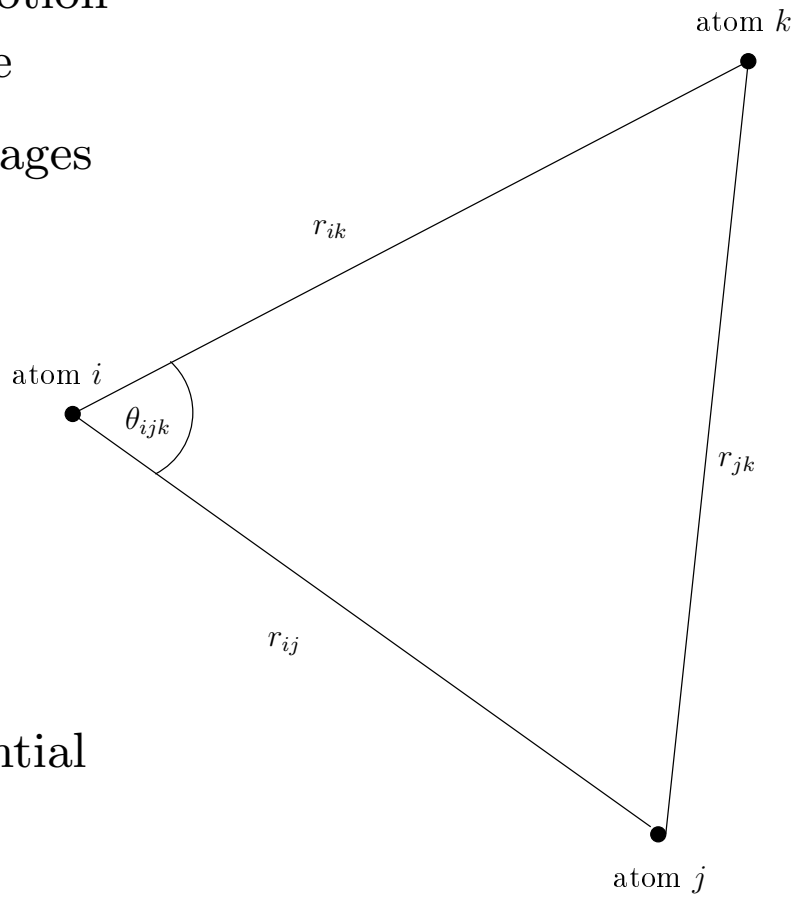

$$E = \frac{1}{2}\sum_{i \neq j} \mathcal{V}_{ij}, \quad \mathcal{V}_{ij} = f_C(r_{ij})\,[f_R(r_{ij}) + b_{ij}\, f_A(r_{ij})]$$

Density functional theory (DFT) calculations

Basic ingredients necessary for DFT

- Hohenberg-Kohn theorem - ground state density $n_0(r)$ ...
  - ... uniquely determines the ground state potential / wavefunctions
  - ... minimizes the systems total energy
- Born-Oppenheimer - N moving electrons in an external potential of static nuclei

$$H\Psi = \left[-\sum_i^N \frac{\hbar^2}{2m}\nabla_i^2 + \sum_i^N V_{\text{ext}}(r_i) + \sum_{i<j}^N V_{e-e}(r_i, r_j) \right] \Psi = E\Psi$$

- Effective potential - averaged electrostatic potential & exchange and correlation

$$V_{\text{eff}}(r) = V_{\text{ext}}(r) + \int \frac{e^2 n(r')}{|r - r'|} d^3r' + V_{\text{XC}}[n(r)]$$

- Kohn-Sham system - Schrödinger equation of N non-interacting particles

$$\left[-\frac{\hbar^2}{2m}\nabla^2 + V_{\text{eff}}(r) \right] \Phi_i(r) = \epsilon_i \Phi_i(r) \quad \Rightarrow \quad n(r) = \sum_i^N |\Phi_i(r)|^2$$

- Self-consistent solution
  $n(r)$ depends on Φ_i, which depend on V_{eff}, which in turn depends on $n(r)$
- Variational principle - minimize total energy with respect to $n(r)$

Density functional theory (DFT) calculations

Details of applied DFT calculations in this work

- Exchange correlation functional - approximations for the inhomogeneous electron gas
  - LDA: $E_{\mathrm{XC}}^{\mathrm{LDA}}[n] = \int \epsilon_{\mathrm{XC}}(n) n(r) d^3r$
  - GGA: $E_{\mathrm{XC}}^{\mathrm{GGA}}[n] = \int \epsilon_{\mathrm{XC}}(n, \nabla n) n(r) d^3r$
- Plane wave basis set - approximation of the wavefunction Φ_i by plane waves φ_j

$$\rightarrow \text{Fourier series: } \Phi_i = \sum_{|G+k|<G_{\mathrm{cut}}} c_j^i \varphi_j(r), \quad E_{\mathrm{cut}} = \frac{\hbar^2}{2m} G_{\mathrm{cut}}^2 \qquad (300 \text{ eV})$$

- Brillouin zone sampling - Γ-point only calculations
- Pseudo potential - consider only the valence electrons
- Code - VASP 4.6

MD and structural optimization

- MD integration: Gear predictor corrector algorithm
- Pressure control: Parrinello-Rahman pressure control
- Structural optimization: Conjugate gradient method

C and Si self-interstitial point defects in silicon

Procedure:

- Creation of c-Si simulation volume
- Periodic boundary conditions
- $T = 0$ K, $p = 0$ bar

↓

Insertion of interstitial C/Si atoms

↓

Relaxation / structural energy minimization

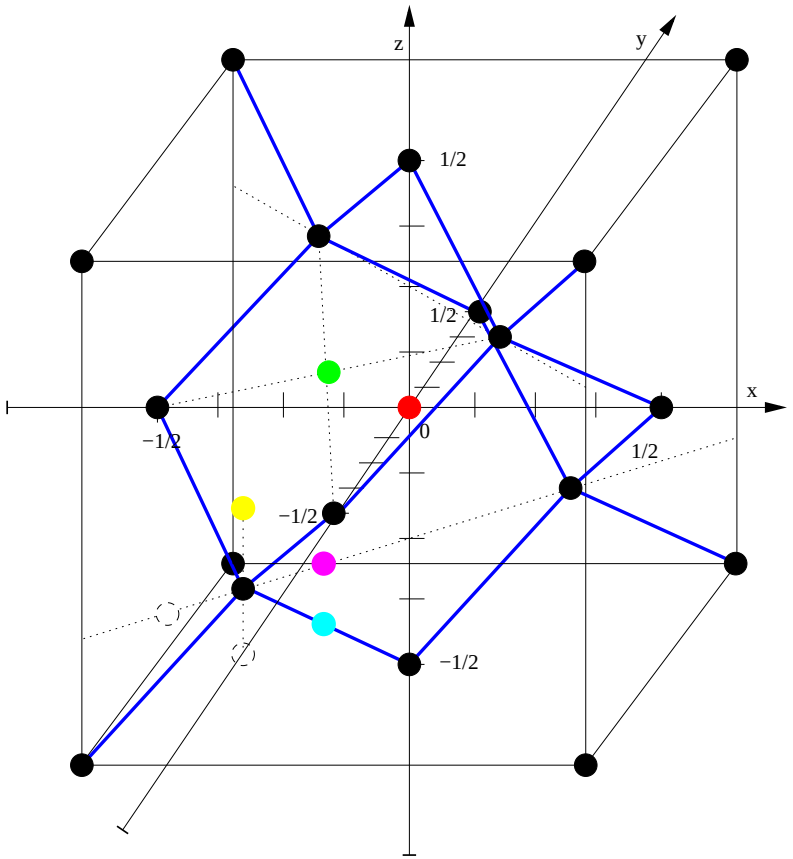

- Tetrahedral
- Hexagonal
- $\langle 1\,0\,0 \rangle$ dumbbell
- $\langle 1\,1\,0 \rangle$ dumbbell
- Bond-centered
- Vacancy / Substitutional

	size [unit cells]	# atoms
VASP	$3 \times 3 \times 3$	216 ± 1
Erhart/Albe	$9 \times 9 \times 9$	5832 ± 1

Si self-interstitial point defects in silicon

E_f [eV]	⟨1 1 0⟩ DB	H	T	⟨1 0 0⟩ DB	V
VASP	3.39	3.42	3.77	4.41	3.63
Erhart/Albe	4.39	4.48*	3.40	5.42	3.13

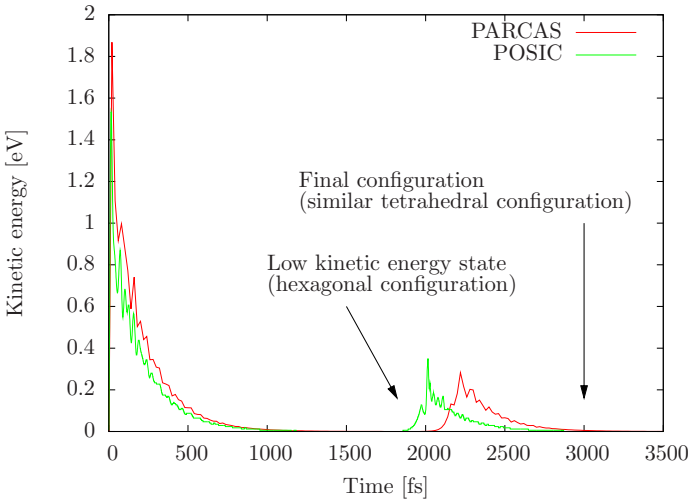

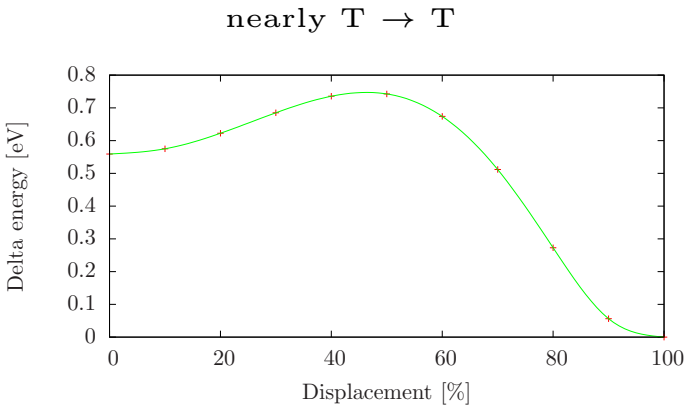

⟨1 1 0⟩ dumbbell

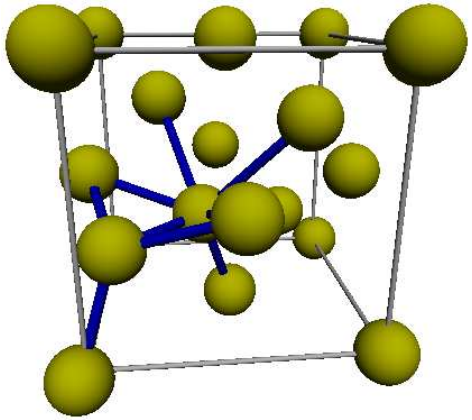

Tetrahedral

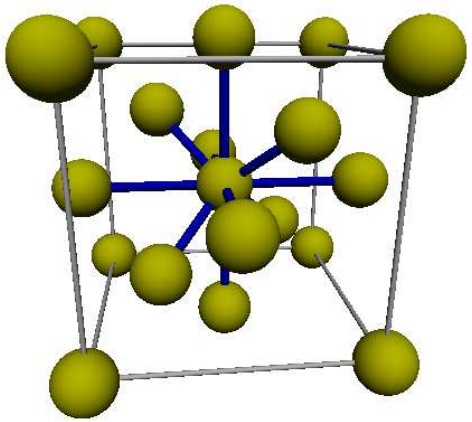

Hexagonal ▷

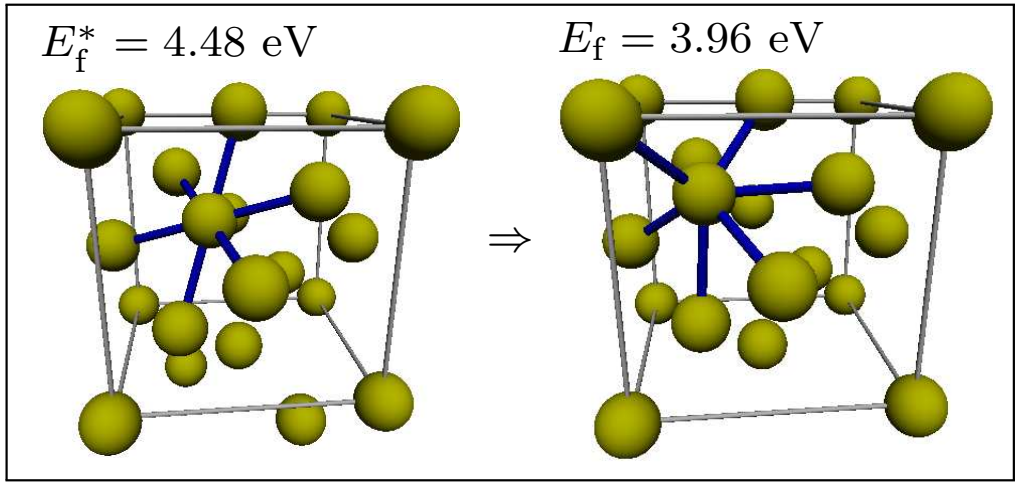

Vacancy

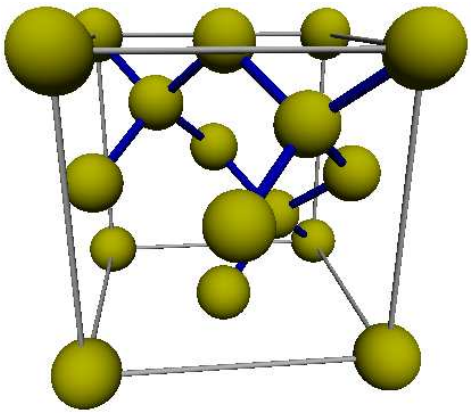

⟨1 0 0⟩ dumbbell

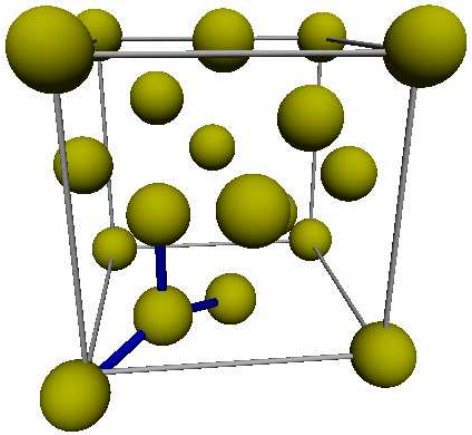

C interstitial point defects in silicon

E_f	T	H	⟨1 0 0⟩ DB	⟨1 1 0⟩ DB	S	B	C_{sub} & Si_i
VASP	unstable	unstable	3.72	4.16	1.95	4.66	4.17
Erhart/Albe MD	6.09	9.05*	3.88	5.18	0.75	5.59*	4.43

Hexagonal ▷
$E_f^* = 9.05$ eV

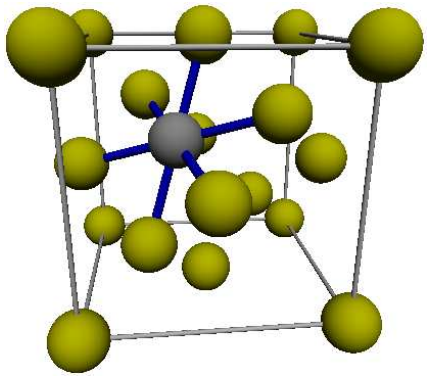

⇒

⟨1 0 0⟩
$E_f = 3.88$ eV

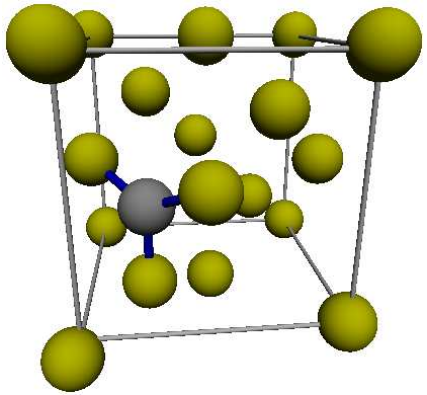

Tetrahedral

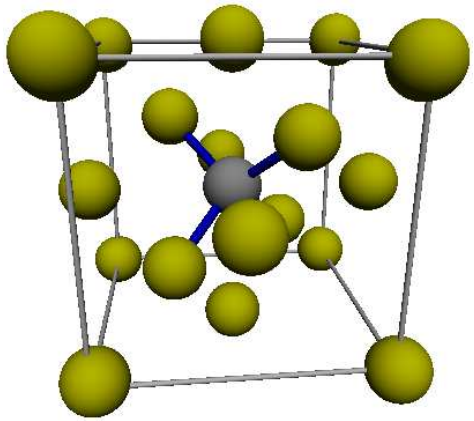

Bond-centered
$E_f^* = 5.59$ eV

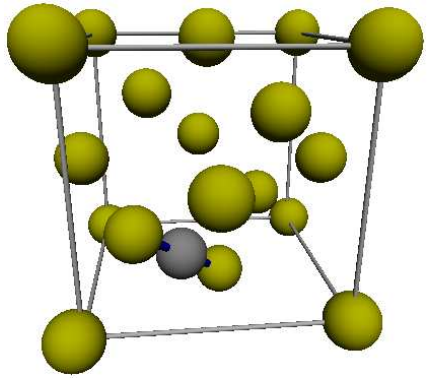

⇒

⟨1 1 0⟩ dumbbell
$E_f = 5.18$ eV

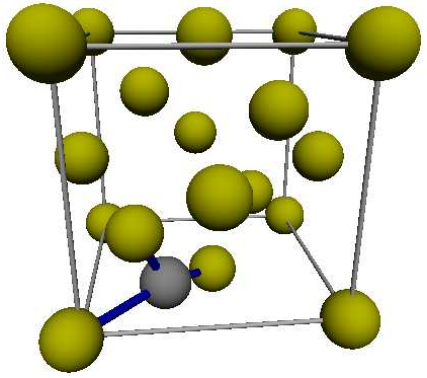

Substitutional

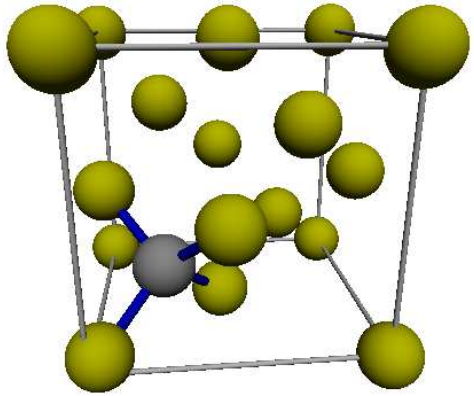

C ⟨1 0 0⟩ dumbbell interstitial configuration

Distances [nm]	$r(1C)$	$r(2C)$	$r(3C)$	$r(12)$	$r(13)$	$r(34)$	$r(23)$	$r(25)$
Erhart/Albe	0.175	0.329	0.186	0.226	0.300	0.343	0.423	0.425
VASP	0.174	0.341	0.182	0.229	0.286	0.347	0.422	0.417

Angles [°]	θ_1	θ_2	θ_3	θ_4
Erhart/Albe	140.2	109.9	134.4	112.8
VASP	130.7	114.4	146.0	107.0

Displacements [nm]	a	b	$\lvert a\rvert + \lvert b\rvert$
Erhart/Albe	0.084	-0.091	0.175
VASP	0.109	-0.065	0.174

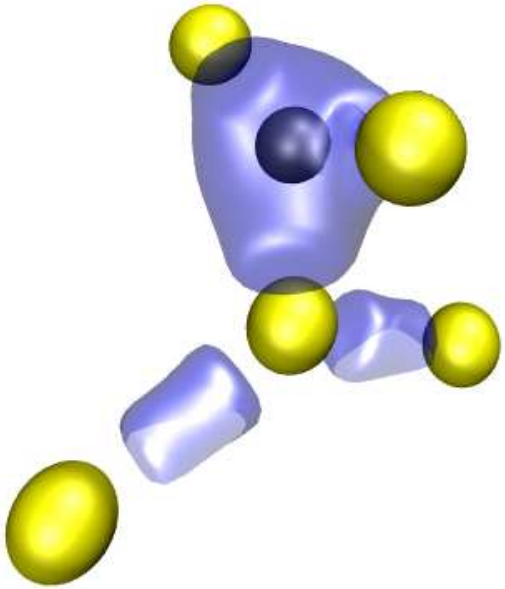

Erhart/Albe

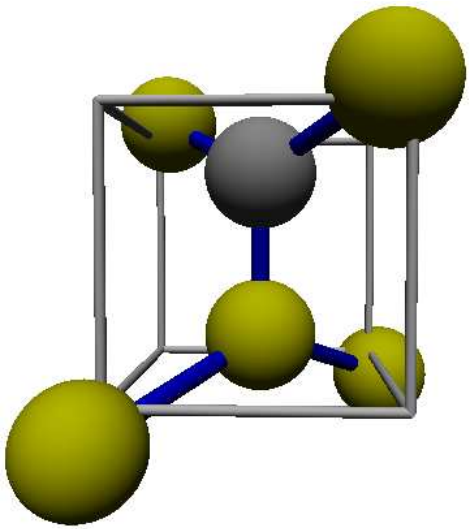

VASP

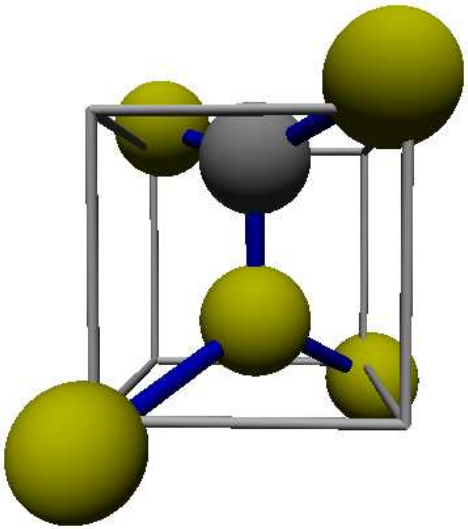

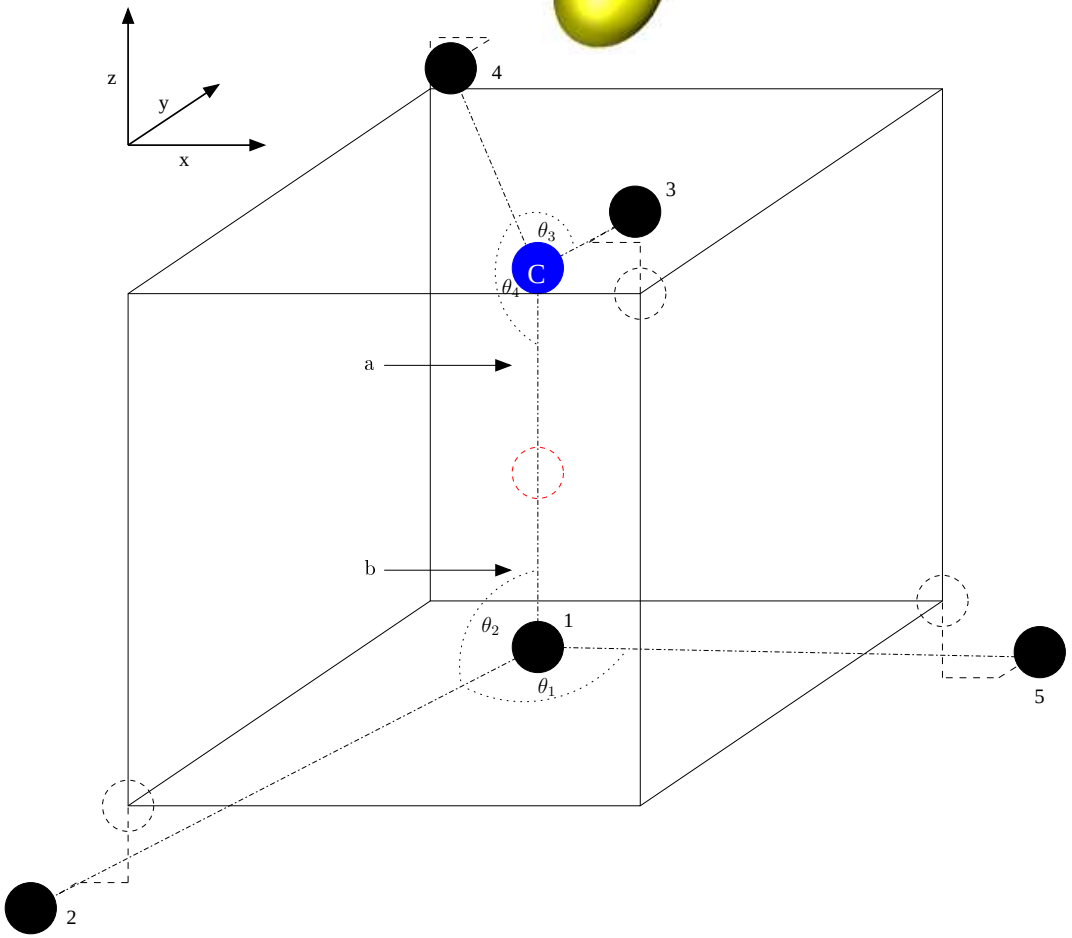

Bond-centered interstitial configuration

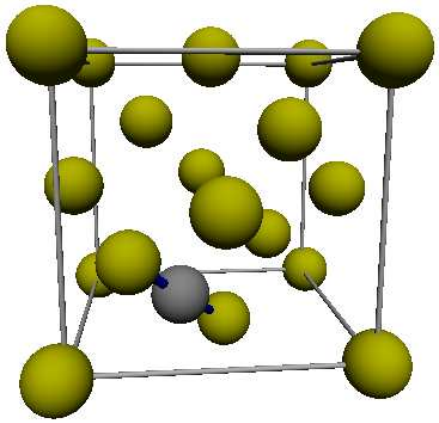

- Linear Si-C-Si bond
- Si: one C & 3 Si neighbours
- Spin polarized calculations
- No saddle point!
  Real local minimum!

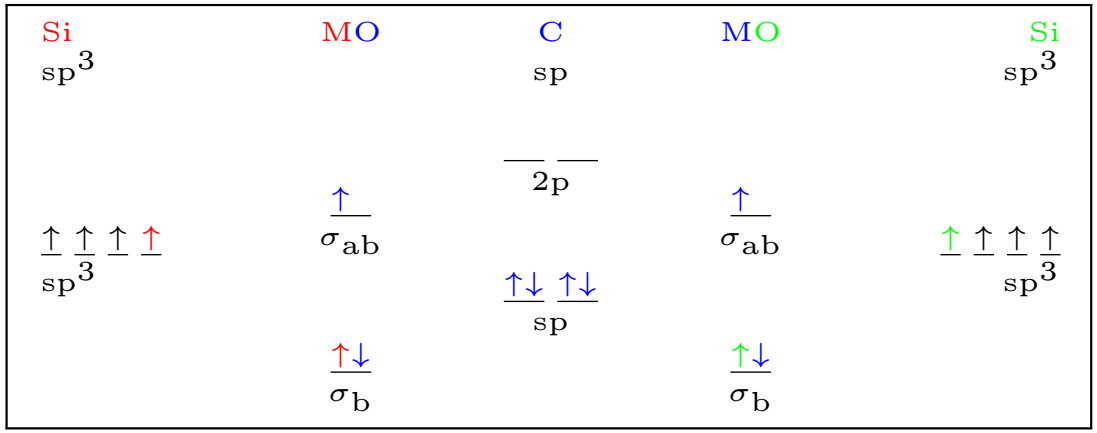

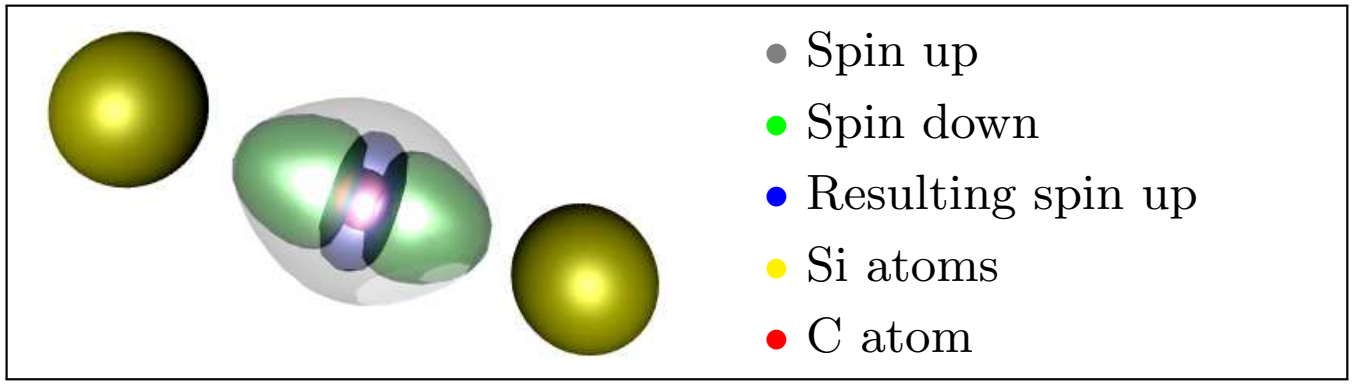

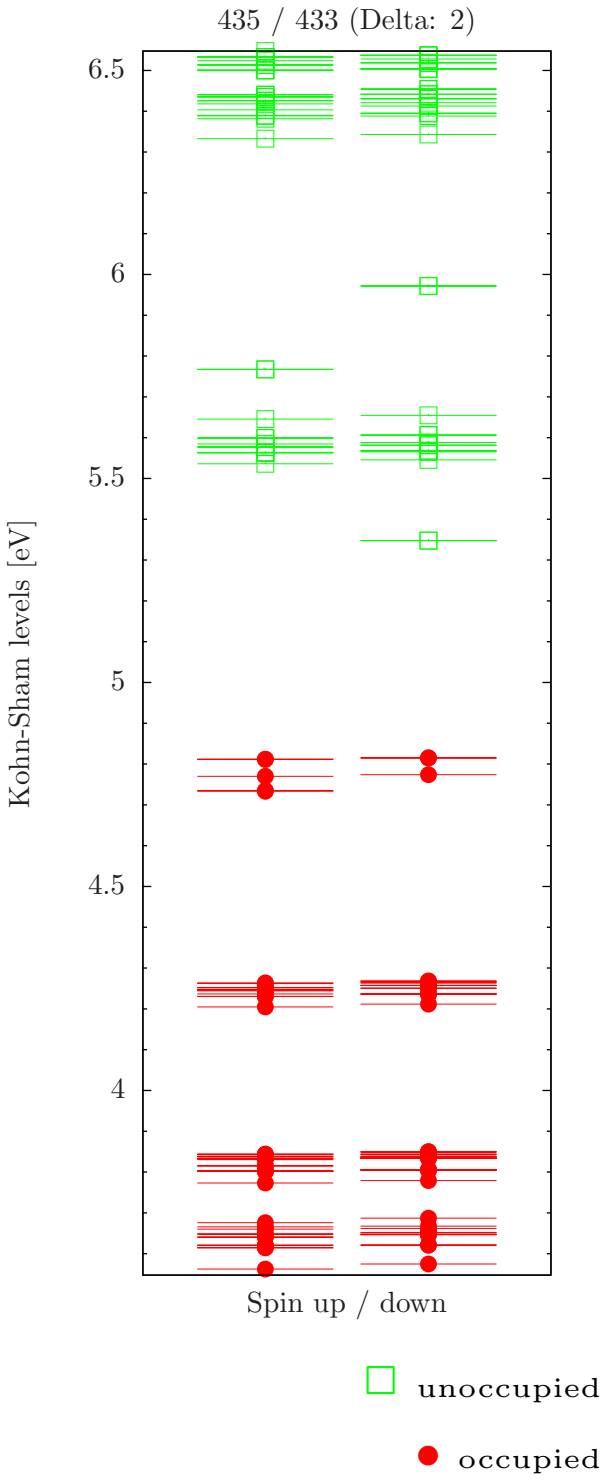

Migration of the C $\langle 1\,0\,0 \rangle$ dumbbell interstitial

Investigated pathways

$\langle 0\,0\,\bar{1} \rangle \rightarrow \langle 0\,0\,1 \rangle$

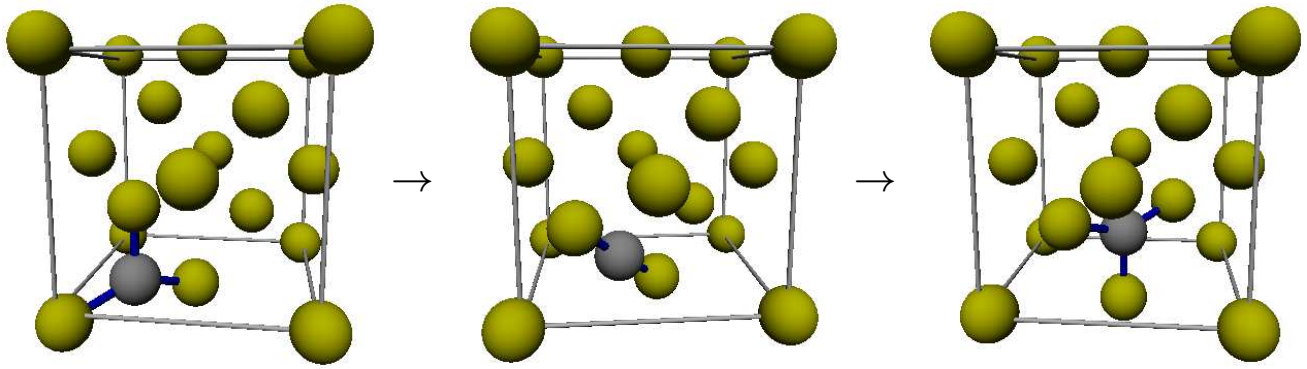

$\langle 0\,0\,\bar{1} \rangle \rightarrow \langle 0\,\bar{1}\,0 \rangle$

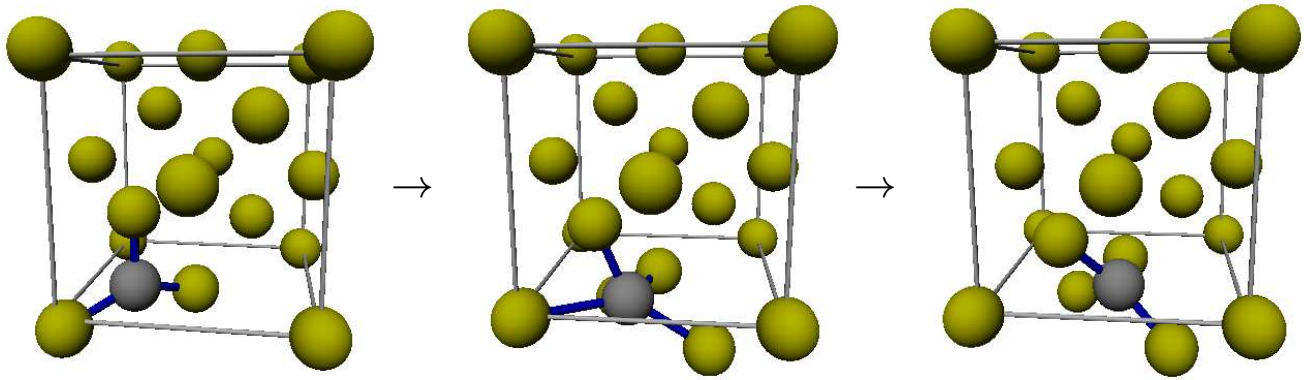

$\langle 0\,0\,\bar{1} \rangle \rightarrow \langle 0\,\bar{1}\,0 \rangle$ (in place)

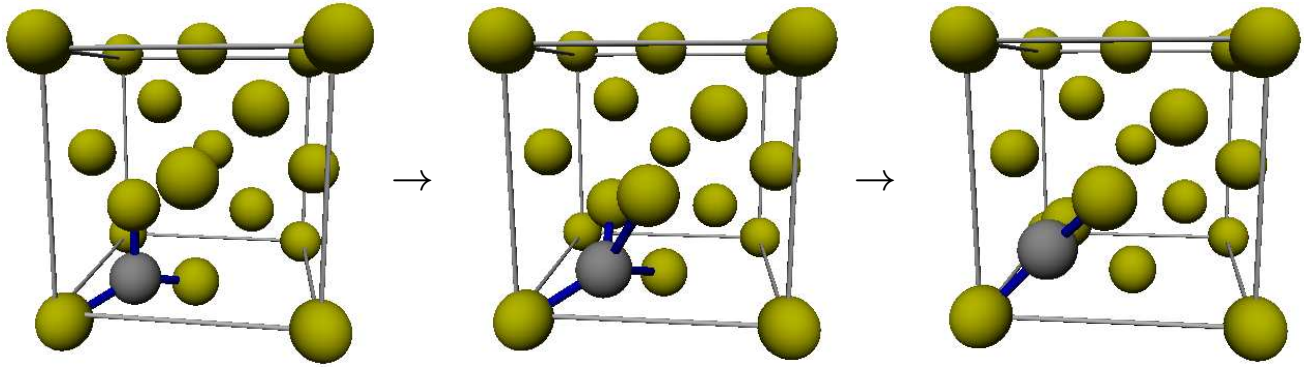

Constrained relaxation technique (CRT) method

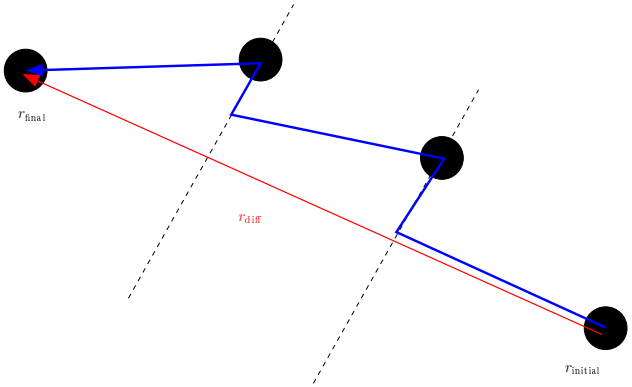

- Constrain diffusing atom
- Static constraints

Modifications

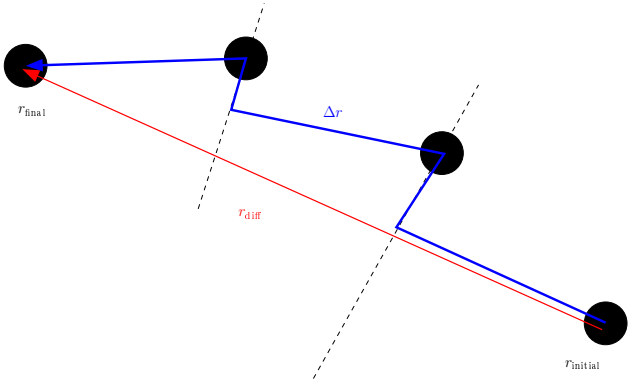

- Constrain all atoms
- Update individual constraints

Migration of the C ⟨1 0 0⟩ dumbbell interstitial

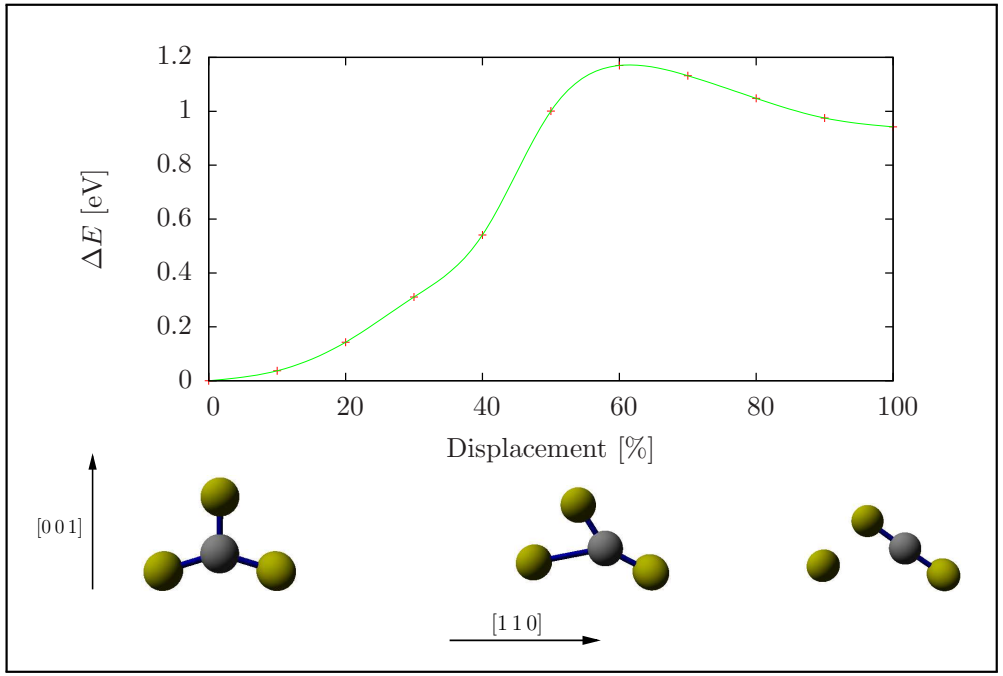

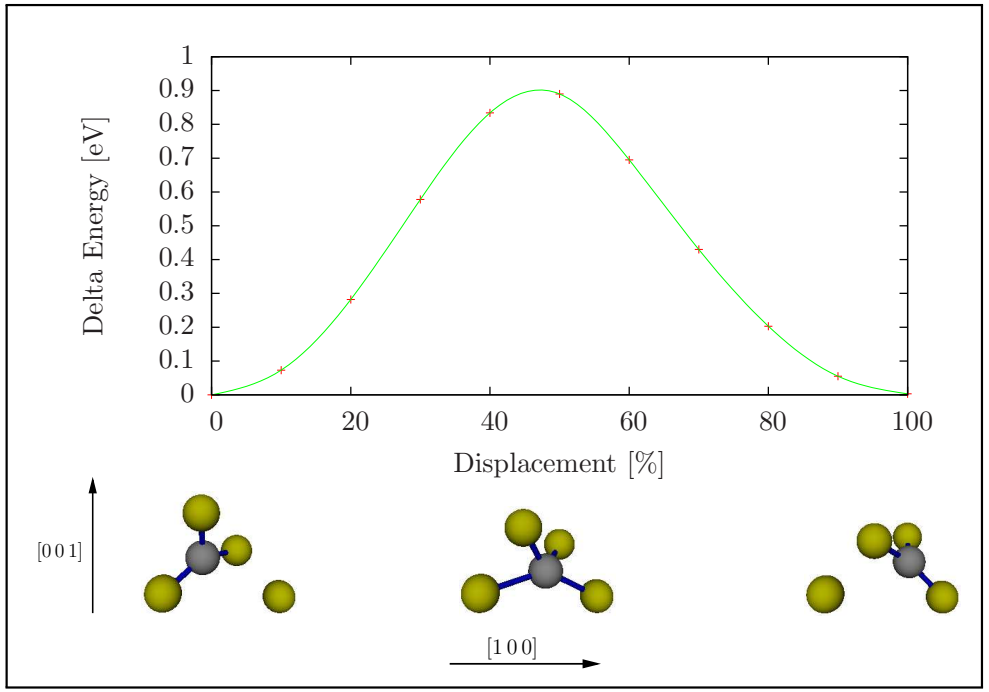

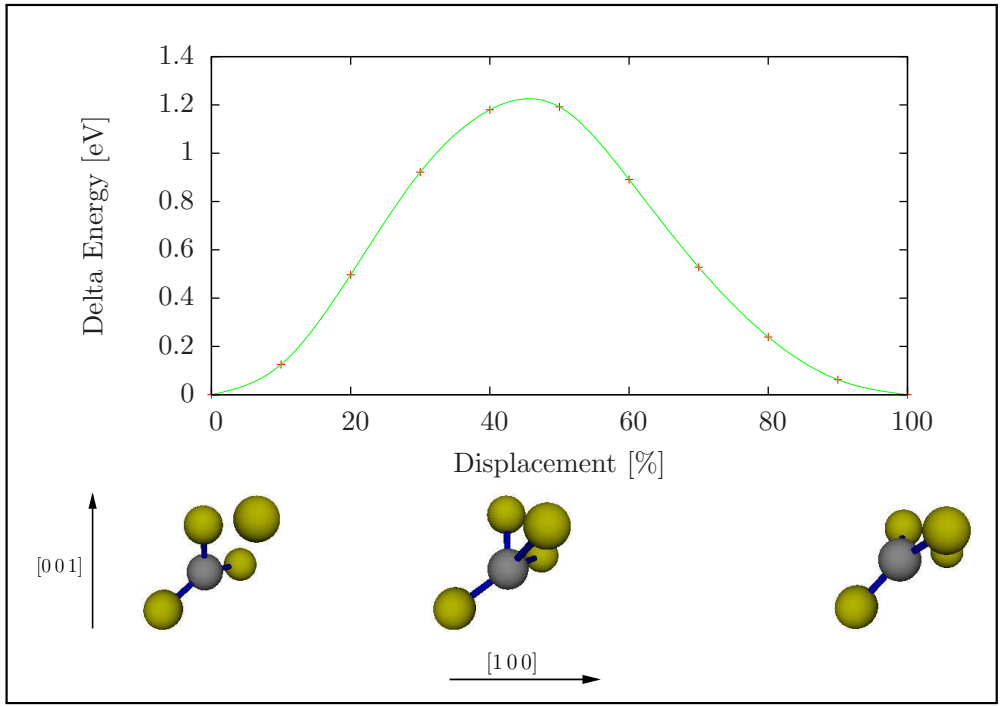

VASP results

- Energetically most favorable path
  - Path 2
  - Activation energy: ≈ 0.9 eV
  - Experimental values: 0.73 ... 0.87 eV

  ⇒ Diffusion path identified!
- Reorientation (path 3)
  - More likely composed of two consecutive steps of type 2
  - Experimental values: 0.77 ... 0.88 eV

  ⇒ Reorientation transition identified!

Migration of the C ⟨1 0 0⟩ dumbbell interstitial

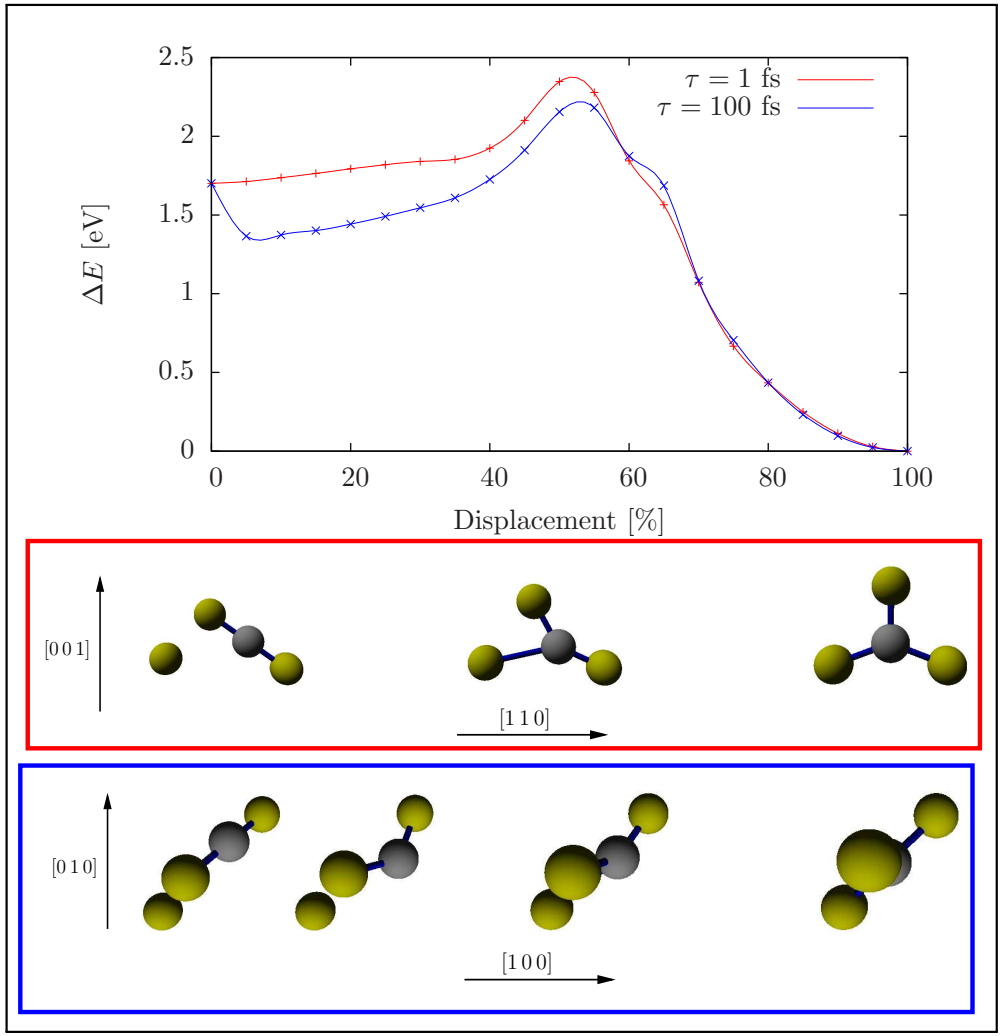

Erhart/Albe results

- Lowest activation energy: ≈ 2.2 eV
- 2.4 times higher than VASP
- Different pathway

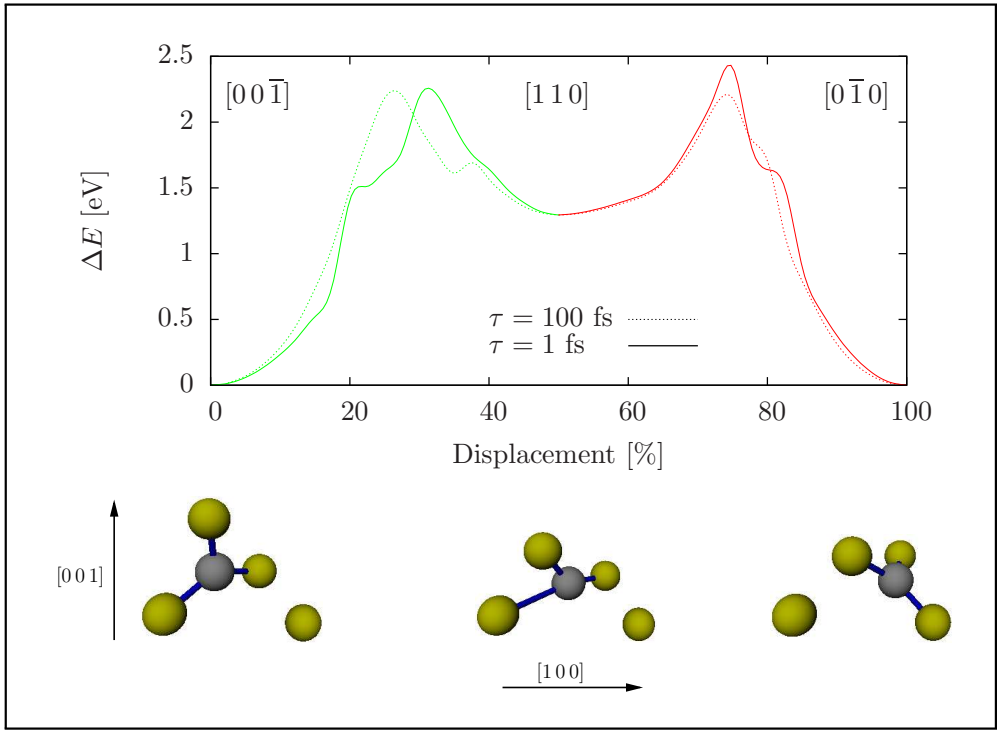

Transition involving C_i ⟨1 1 0⟩

- Bond-centered configuration unstable
  → C_i ⟨1 1 0⟩ dumbbell
- Transition minima of path 2 & 3
  → C_i ⟨1 1 0⟩ dumbbell
- Activation energy: ≈ 2.2 eV & 0.9 eV
- 2.4 - 3.4 times higher than VASP
- Rotation of dumbbell orientation

Overestimated diffusion barrier

Combinations with a C-Si $\langle 1\,0\,0\rangle$-type interstitial

Binding energy: $E_\mathrm{b} = E_\mathrm{f}^{\text{defect combination}} - E_\mathrm{f}^{\text{C } \langle 0\,0\,\bar{1}\rangle \text{ dumbbell}} - E_\mathrm{f}^{\text{2nd defect}}$

E_b [eV]	1	2	3	4	5	R
$\langle 0\,0\,\bar{1}\rangle$	-0.08	-1.15	-0.08	0.04	-1.66	-0.19
$\langle 0\,0\,1\rangle$	0.34	0.004	-2.05	0.26	-1.53	-0.19
$\langle 0\,\bar{1}\,0\rangle$	-2.39	-0.17	-0.10	-0.27	-1.88	-0.05
$\langle 0\,1\,0\rangle$	-2.25	-1.90	-2.25	-0.12	-1.38	-0.06
$\langle \bar{1}\,0\,0\rangle$	-2.39	-0.36	-2.25	-0.12	-1.88	-0.05
$\langle 1\,0\,0\rangle$	-2.25	-2.16	-0.10	-0.27	-1.38	-0.06
C substitutional (C_S)	0.26	-0.51	-0.93	-0.15	0.49	-0.05
Vacancy	-5.39 ($\rightarrow C_S$)	-0.59	-3.14	-0.54	-0.50	-0.31

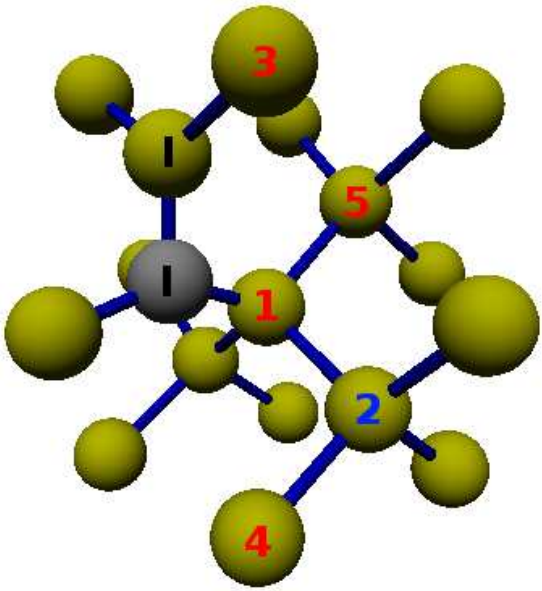

$\langle 1\,0\,0\rangle$ at position 1

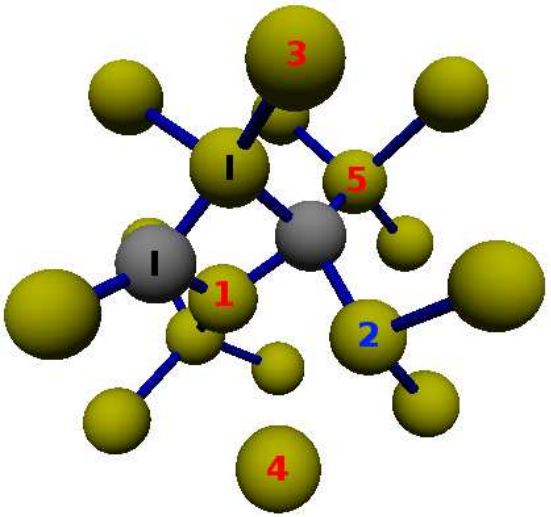

$\langle 0\,\bar{1}\,0\rangle$ at position 1

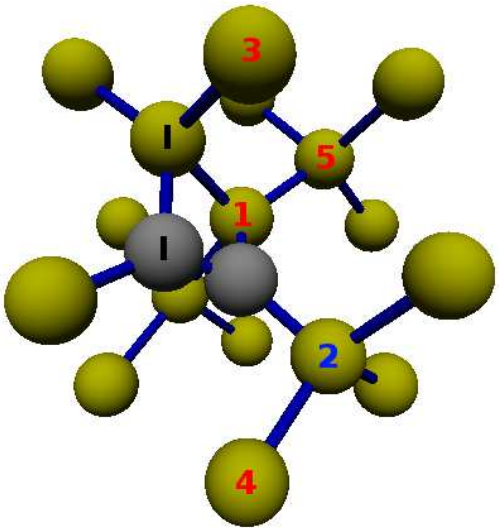

- $E_\mathrm{b} = 0 \Leftrightarrow$ non-interacting defects
  $E_\mathrm{b} \rightarrow 0$ for increasing distance (R)
- Stress compensation / increase
- Unfavored: antiparallel orientations
- Indication of energetically favored agglomeration
- Most favorable: C clustering
- However: High barrier ($> 4\,\mathrm{eV}$)
- 4×-2.25 versus 2×-2.39 (Entropy)

Combinations of C-Si $\langle 1\,0\,0\rangle$-type interstitials

Energetically most favorable combinations along $\langle 1\,1\,0\rangle$

	1	2	3	4	5	6
E_b [eV]	-2.39	-1.88	-0.59	-0.31	-0.24	-0.21
C-C distance [Å]	1.4	4.6	6.5	8.6	10.5	10.8
Type	$\langle\bar{1}\,0\,0\rangle$	$\langle 1\,0\,0\rangle$	$\langle 1\,0\,0\rangle$	$\langle 1\,0\,0\rangle$	$\langle 1\,0\,0\rangle$	$\langle 1\,0\,0\rangle$, $\langle 0\,\bar{1}\,0\rangle$

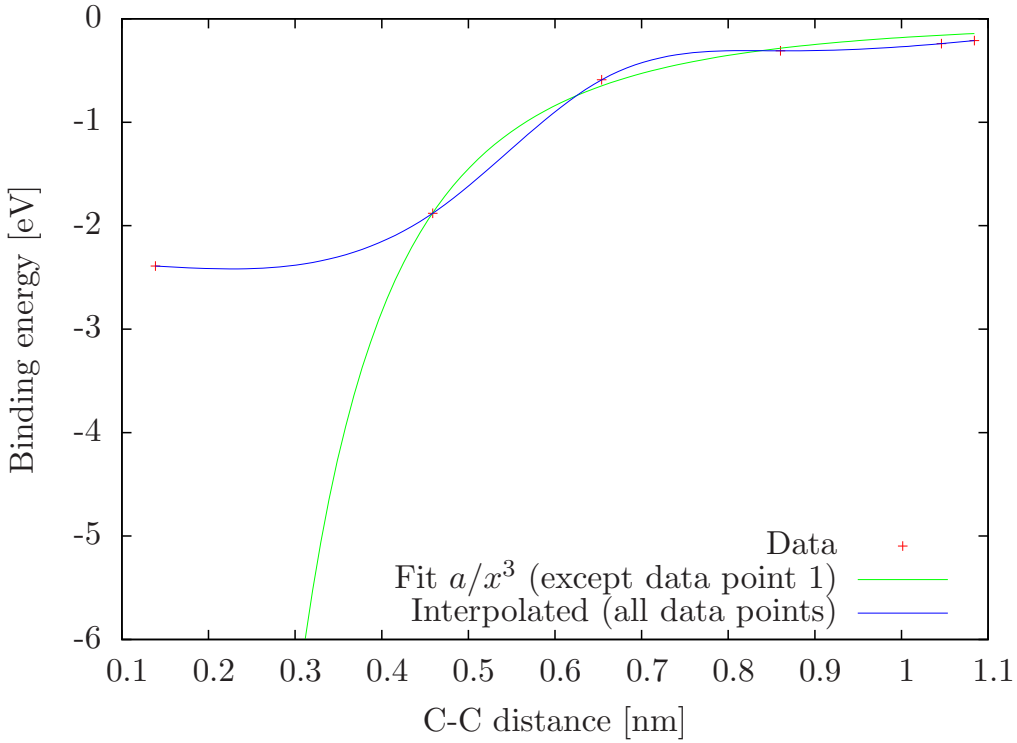

- Interaction proportional to reciprocal cube of C-C distance
- Saturation in the immediate vicinity

$\Rightarrow$ Agglomeration of $\mathrm{C_i}$ expected

$\Rightarrow$ Absence of C clustering

Consisten with initial precipitation model

Combinations of substitutional C and ⟨1 1 0⟩ Si self-interstitials

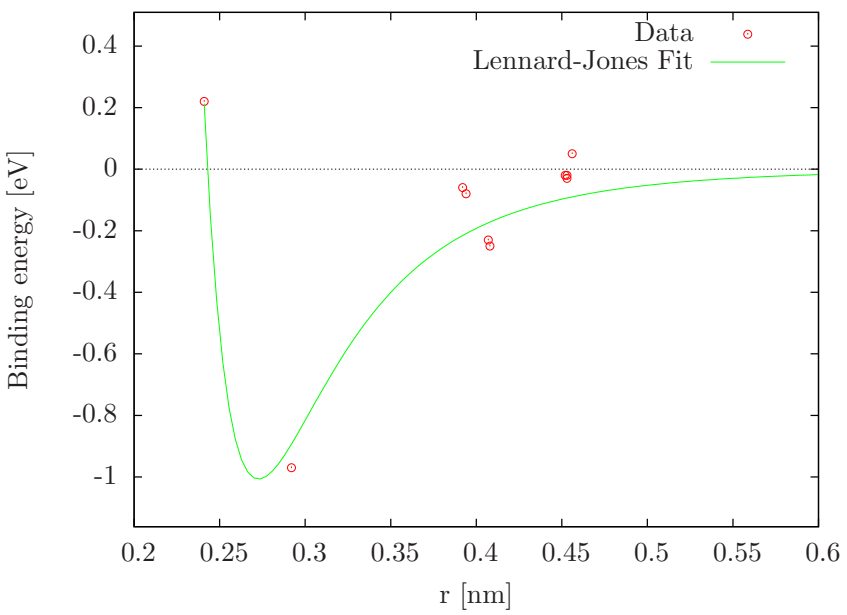

- IBS: C may displace Si
  $\Rightarrow$ C_{sub} + ⟨1 1 0⟩ Si self-interstitial
- Assumption:
  ⟨1 1 0⟩-type $\rightarrow$ favored combination

$\Rightarrow$ Most favorable: C_{sub} along ⟨1 1 0⟩ chain Si_i

$\Rightarrow$ Less favorable than C-Si ⟨1 0 0⟩ dumbbell

$\Rightarrow$ Interaction drops quickly to zero
$\rightarrow$ low capture radius

IBS process far from equilibrium
C_{sub} & Si_i instead of thermodynamic ground state

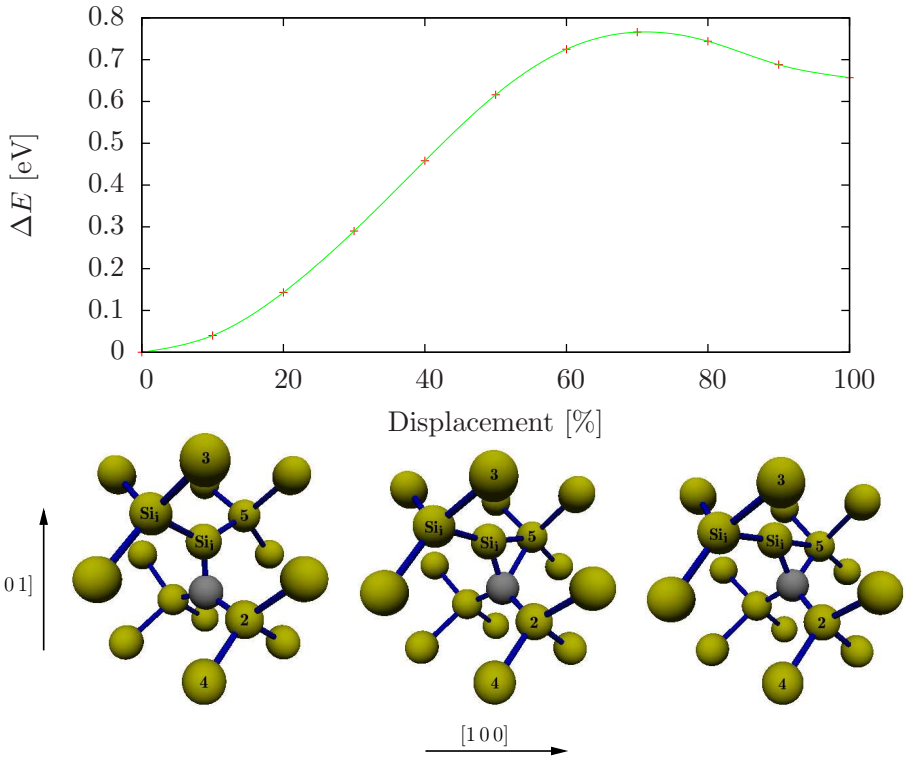

Ab initio MD at 900 °C

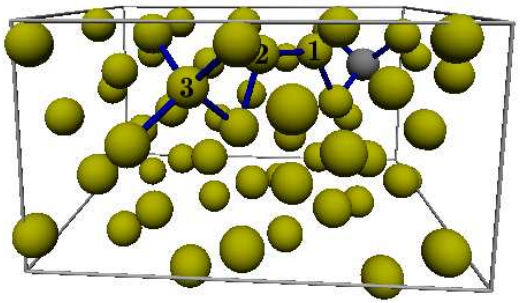

$t = 2230$ fs

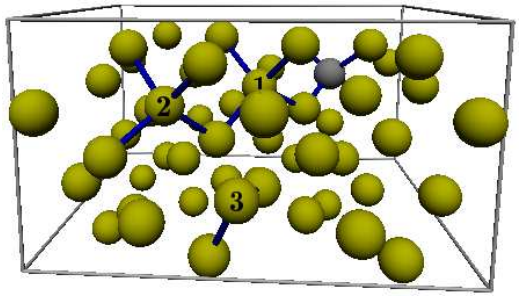

$t = 2900$ fs

Contribution of entropy to structural formation

Migration in C-Si $\langle 1\,0\,0 \rangle$ and vacancy combinations

Pos 2, $E_\mathrm{b} = -0.59$ eV

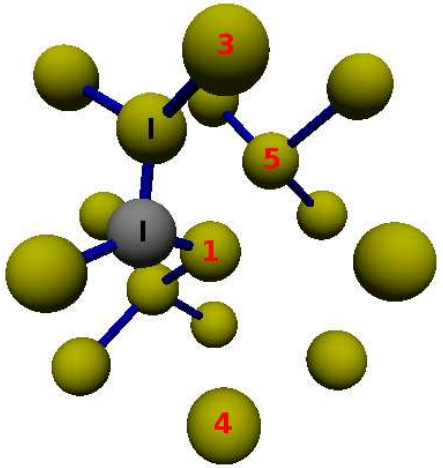

Low activation energies

High activation energies for reverse processes

$\Downarrow$

C_{sub} very stable

Without nearby $\langle 1\,1\,0 \rangle$ Si self-interstitial (IBS)

$\Downarrow$

Formation of SiC by successive substitution by C

Pos 3, $E_\mathrm{b} = -3.14$ eV

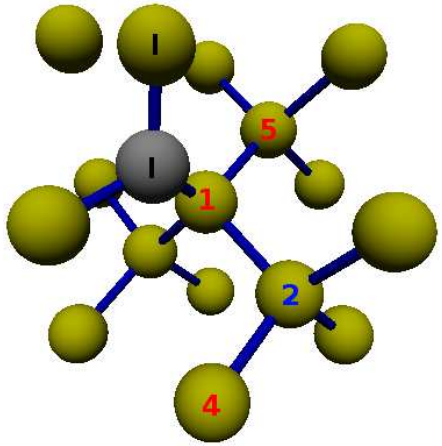

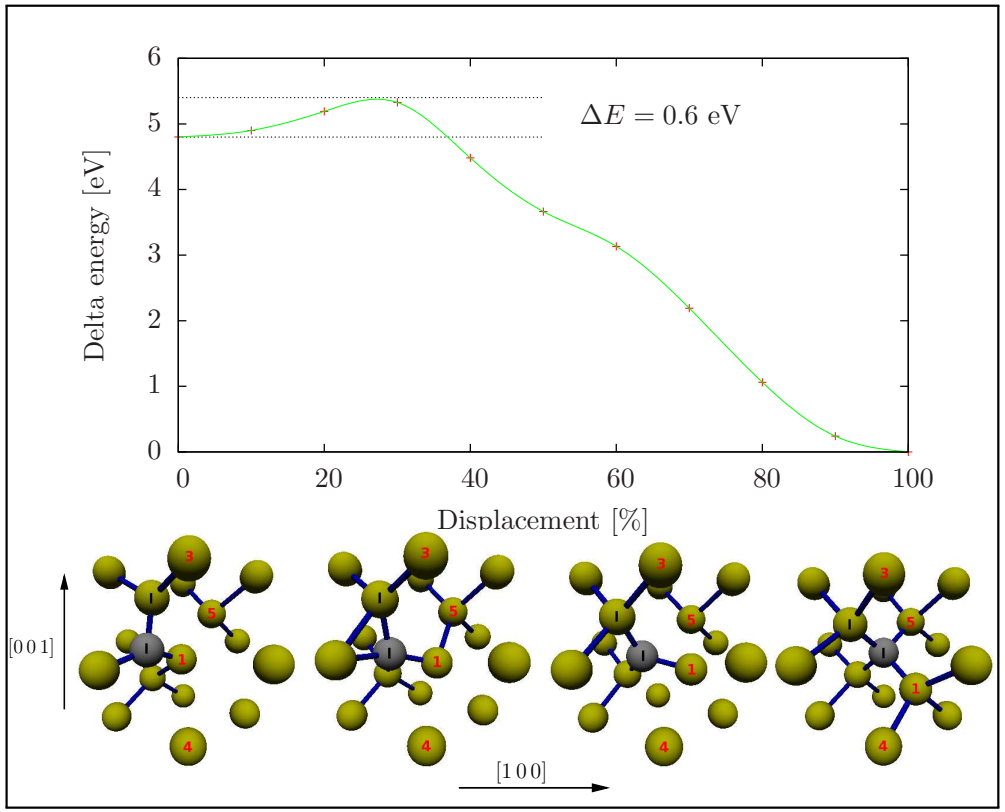

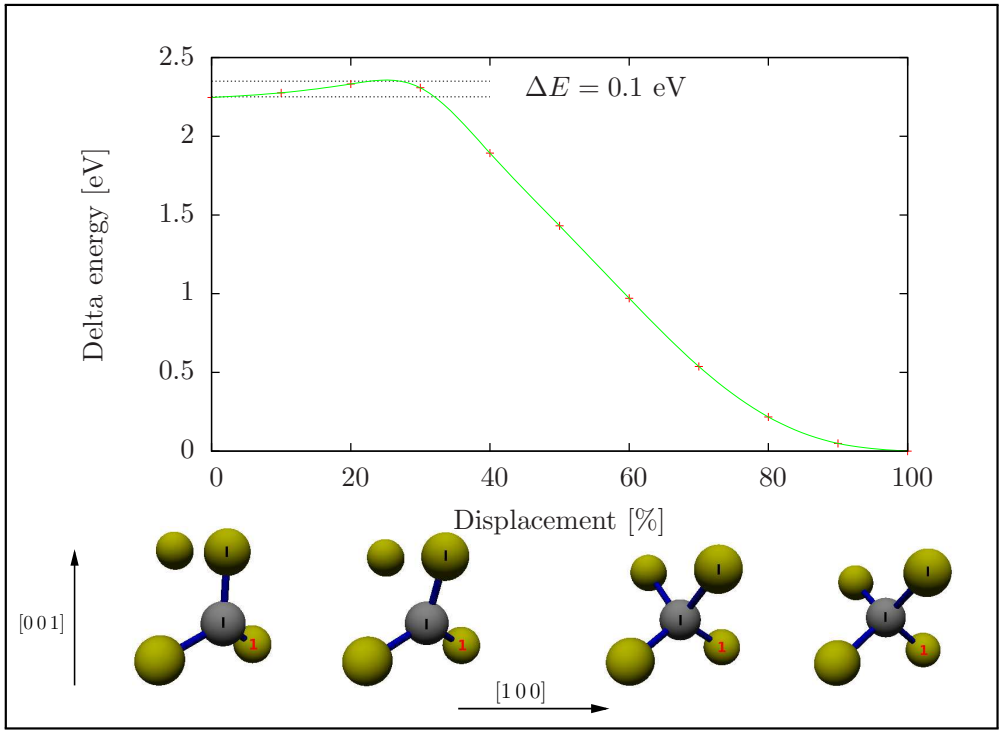

Conclusion of defect / migration / combined defect simulations

Defect structures

- Accurately described by quantum-mechanical simulations
- Less accurate description by classical potential simulations
- Underestimated formation energy of C_{sub} by classical approach
- Both methods predict same ground state: C_i $\langle 1\,0\,0 \rangle$ dumbbell

Migration

- C migration pathway in Si identified
- Consistent with reorientation and diffusion experiments
- Different path and ...
- overestimated barrier by classical potential calculations

Concerning the precipitation mechanism

- Agglomeration of C-Si dumbbells energetically favorable (stress compensation)
- C-Si indeed favored compared to C_{sub} & $\langle 1\,1\,0 \rangle$ Si self-interstitial
- Possible low interaction capture radius of C_{sub} & $\langle 1\,1\,0 \rangle$ Si self-interstitial
- Low barrier for C_i $\langle 1\,0\,0 \rangle \rightarrow C_{sub}$ & Si_i $\langle 1\,1\,0 \rangle$
- In absence of nearby $\langle 1\,1\,0 \rangle$ Si self-interstitial: C-Si $\langle 1\,0\,0 \rangle$ + Vacancy $\rightarrow C_{sub}$ (SiC)

Results suggest increased participation of C_{sub}

Silicon carbide precipitation simulations

- Create c-Si volume
- Periodc boundary conditions
- Set requested T and $p = 0$ bar
- Equilibration of E_{kin} and E_{pot}

Insertion of C atoms at constant T

- total simulation volume
- volume of minimal SiC precipitate
- volume consisting of Si atoms to form a minimal precipitate

Run for 100 ps followed by cooling down to 20 °C

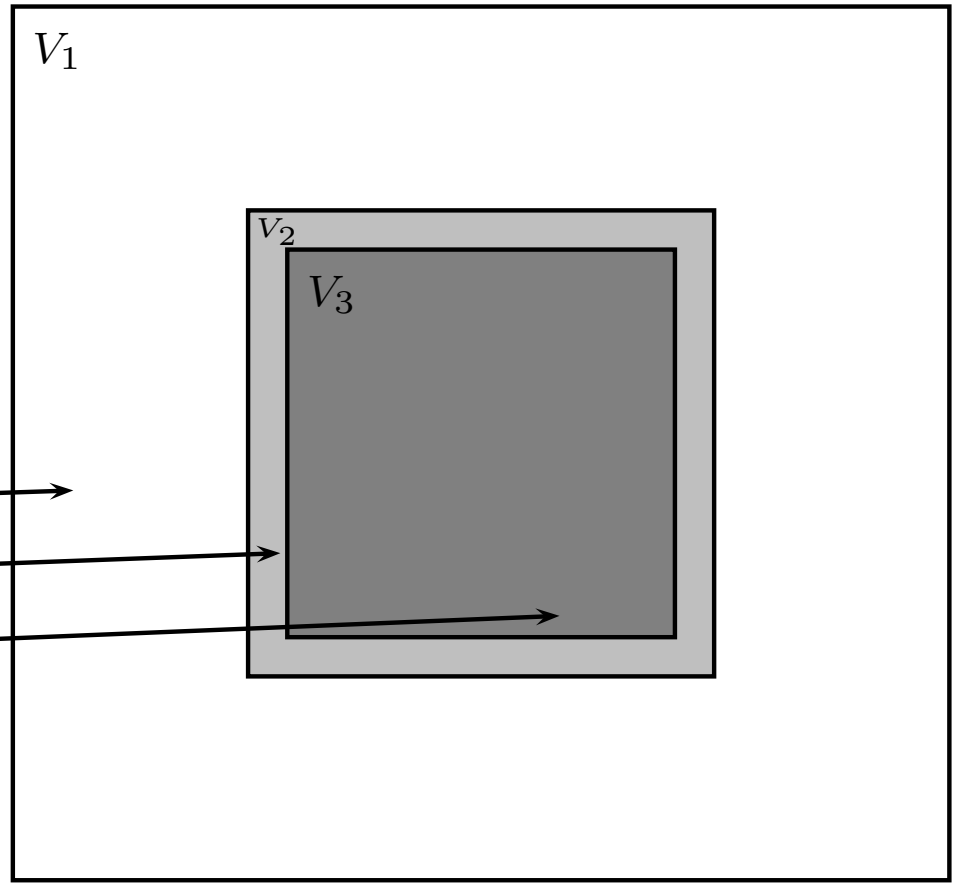

- Restricted to classical potential simulations
- V_2 and V_3 considered due to low diffusion
- Amount of C atoms: 6000 ($r_{\text{prec}} \approx 3.1$ nm, IBS: 2 ... 4 nm)
- Simulation volume: $31 \times 31 \times 31$ unit cells (238328 Si atoms)

Silicon carbide precipitation simulations at 450 °C as in IBS

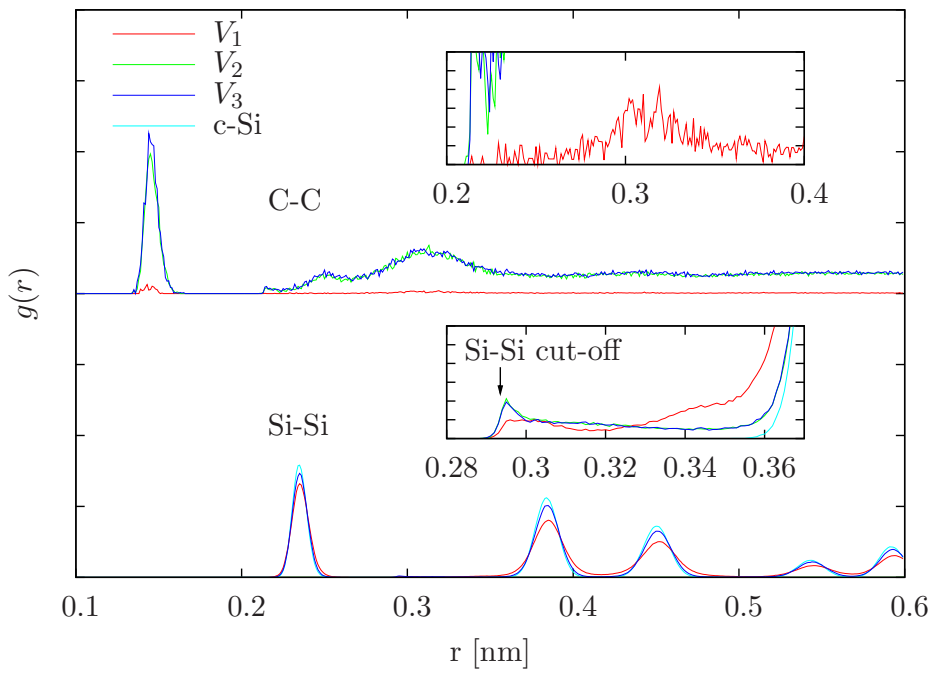

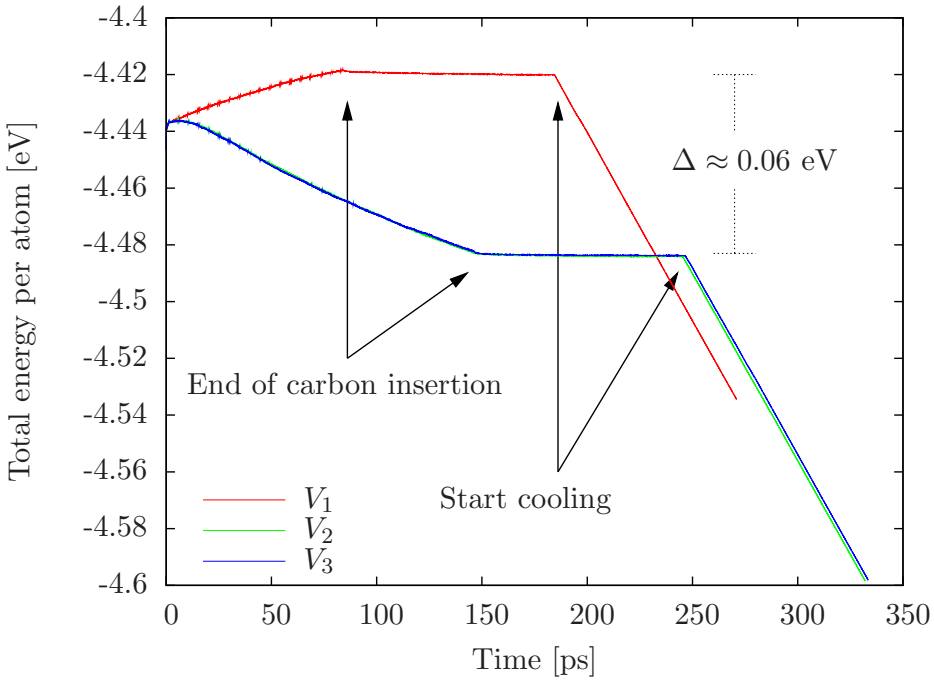

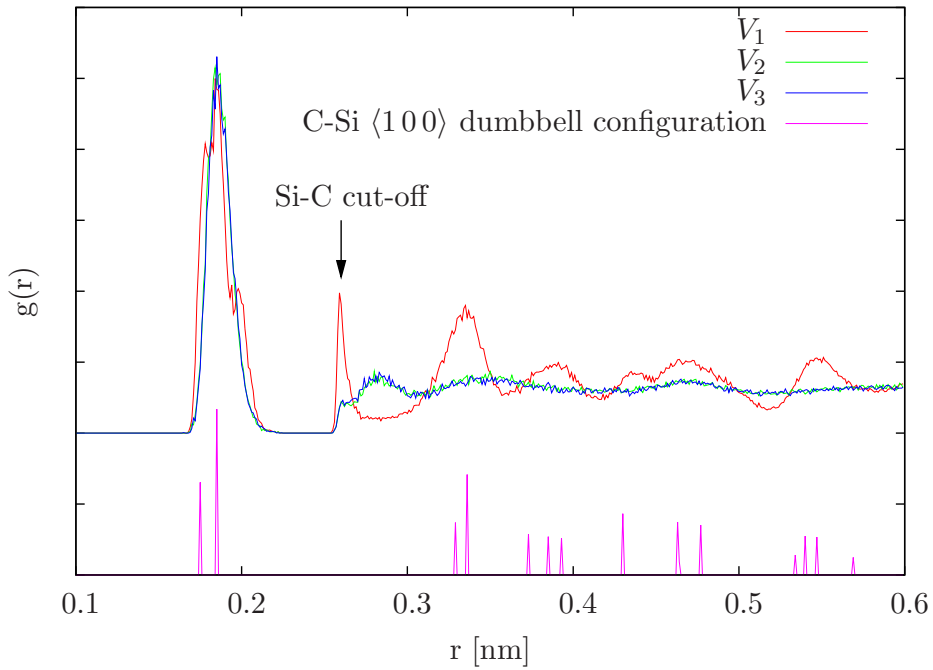

Low C concentration (V_1)

⟨1 0 0⟩ C-Si dumbbell dominated structure

- Si-C bumbs around 0.19 nm
- C-C peak at 0.31 nm (as expected in 3C-SiC): concatenated dumbbells of various orientation
- Si-Si NN distance stretched to 0.3 nm

⇒ C atoms in proper 3C-SiC distance first

High C concentration (V_2, V_3)

High amount of strongly bound C-C bonds

Defect density ↑ ⇒ considerable amount of damage

Only short range order observable

⇒ amorphous SiC-like phase

Silicon carbide precipitation simulations at 450 °C as in IBS

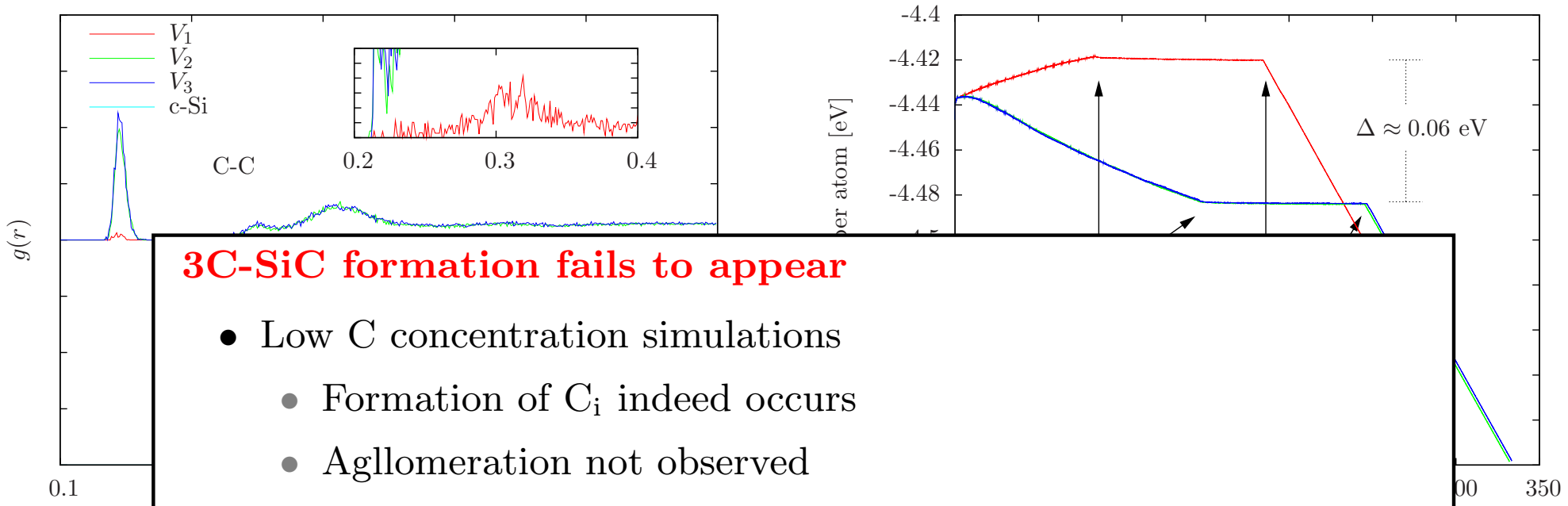

3C-SiC formation fails to appear

- Low C concentration simulations
  - Formation of C_i indeed occurs
  - Agllomeration not observed
- High C concentration simulations
  - Amorphous SiC-like structure (not expected at prevailing temperatures)
  - Rearrangement and transition into 3C-SiC structure missing

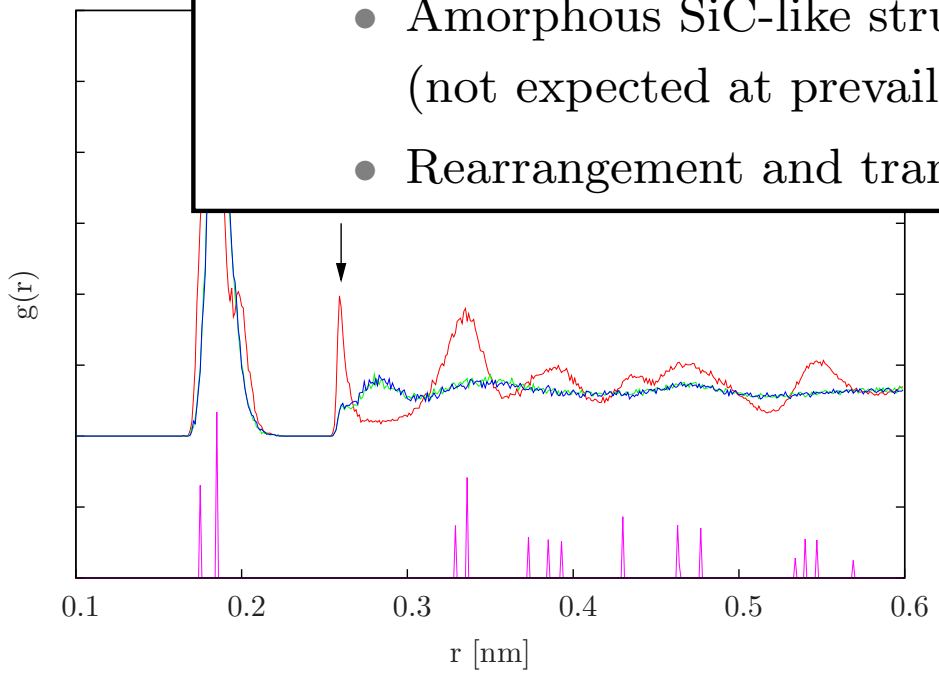

3C-SiC):
concatenated dumbbells of various orientation

- Si-Si NN distance stretched to 0.3 nm

⇒ C atoms in proper 3C-SiC distance first

High C concentration (V_2, V_3)

High amount of strongly bound C-C bonds

Defect density ↑ ⇒ considerable amount of damage

Only short range order observable

⇒ amorphous SiC-like phase

Limitations of molecular dynamics and short range potentials

Time scale problem of MD

Minimize integration error
⇒ discretization considerably smaller than reciprocal of fastest vibrational mode

Order of fastest vibrational mode: $10^{13} - 10^{14}$ Hz
⇒ suitable choice of time step: $\tau = 1$ fs $= 10^{-15}$ s
⇒ slow phase space propagation

Several local minima in energy surface separated by large energy barriers
⇒ transition event corresponds to a multiple of vibrational periods
⇒ phase transition made up of many infrequent transition events

Accelerated methods: Temperature accelerated MD (TAD), self-guided MD ...

retain proper thermodynmic sampling

Limitations related to the short range potential

Cut-off function pushing forces and energies to zero between 1^{st} and 2^{nd} next neighbours
⇒ overestimated unphysical high forces of next neighbours

Potential enhanced problem of slow phase space propagation

Approach to the (twofold) problem

Increased temperature simulations without TAD corrections
(accelerated methods or higher time scales exclusively not sufficient)

IBS

- 3C-SiC also observed for higher T
- higher T inside sample
- structural evolution vs. equilibrium properties

Increased temperature simulations at low C concentration

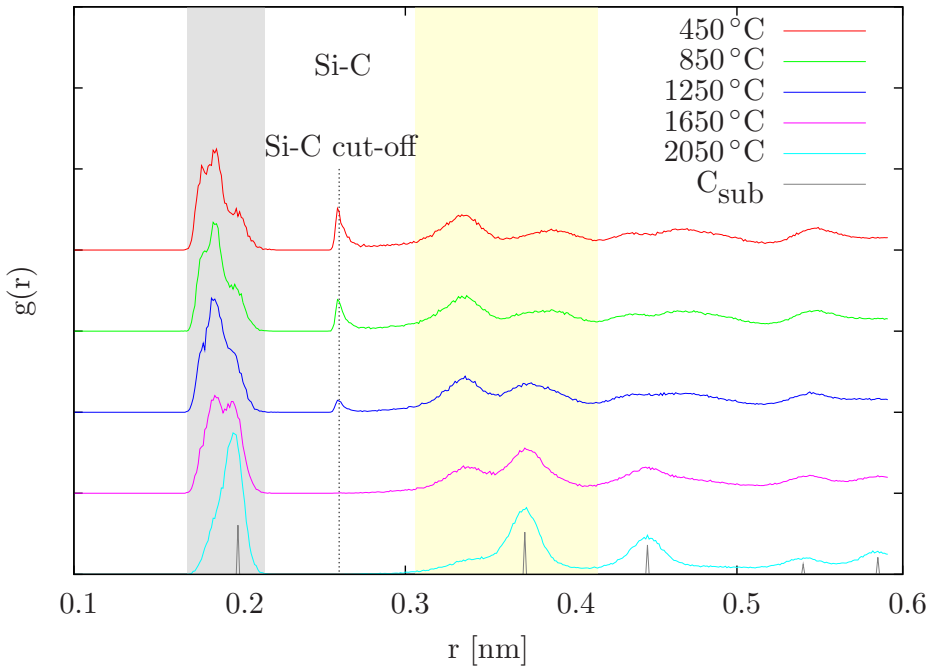

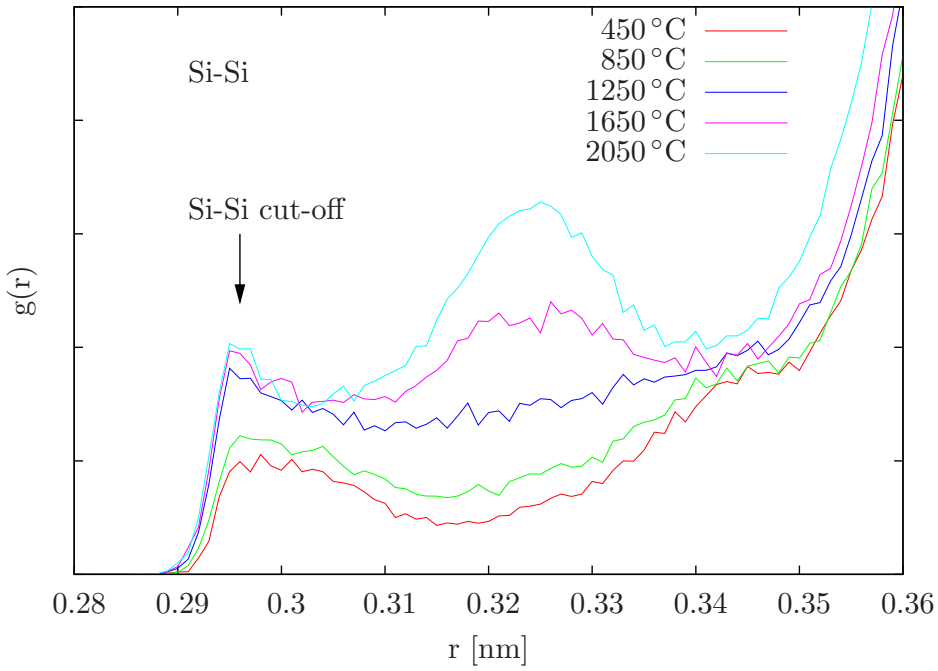

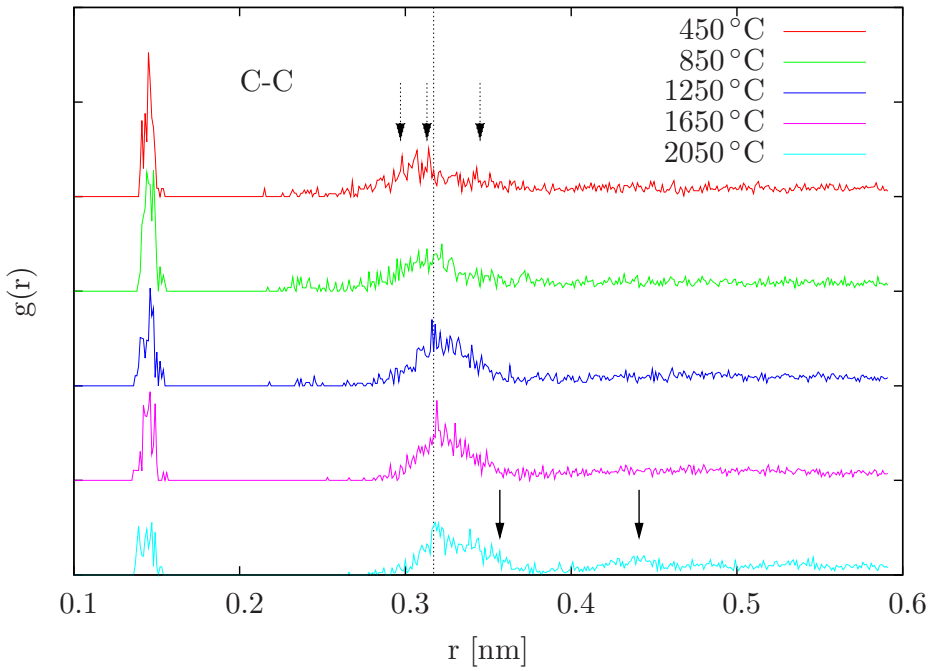

Si-C bonds:

- Vanishing cut-off artifact (above 1650 °C)
- Structural change: C-Si $\langle 1\,0\,0 \rangle \rightarrow C_{sub}$

Si-Si bonds: Si-C_{sub}-Si along $\langle 1\,1\,0 \rangle$ ($\rightarrow$ 0.325 nm)

stretched SiC in c-Si

C-C bonds:

- C-C next neighbour pairs reduced (mandatory)
- Peak at 0.3 nm slightly shifted
  - C-Si $\langle 1\,0\,0 \rangle$ combinations (dashed arrows)
    $\rightarrow$ C-Si $\langle 1\,0\,0 \rangle$ & C_{sub} combinations (|)
    $\rightarrow$ pure C_{sub} combinations (↓)
  - Range [|-↓]: C_{sub} & C_{sub} with nearby Si_I

Increased temperature simulations at low C concentration

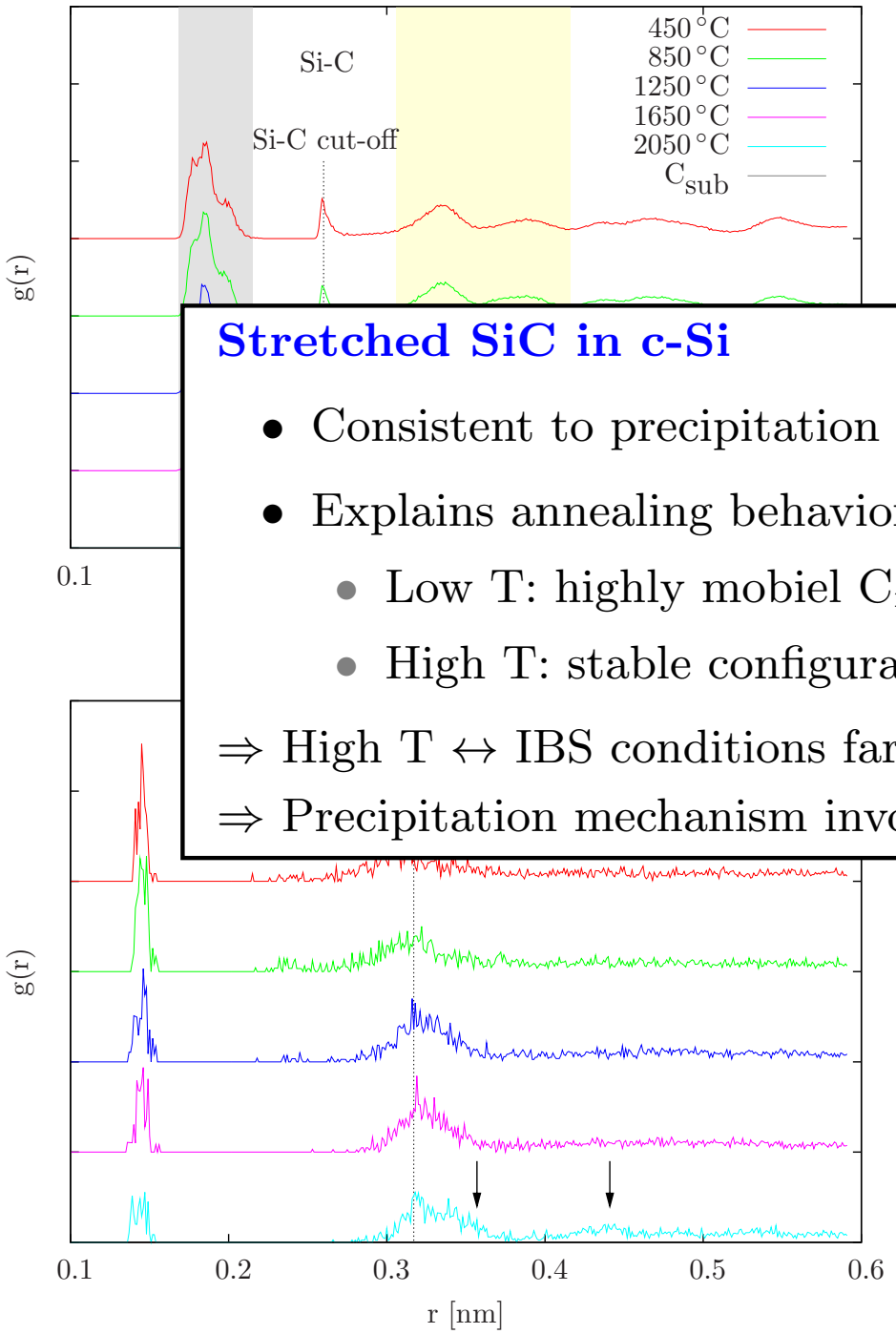

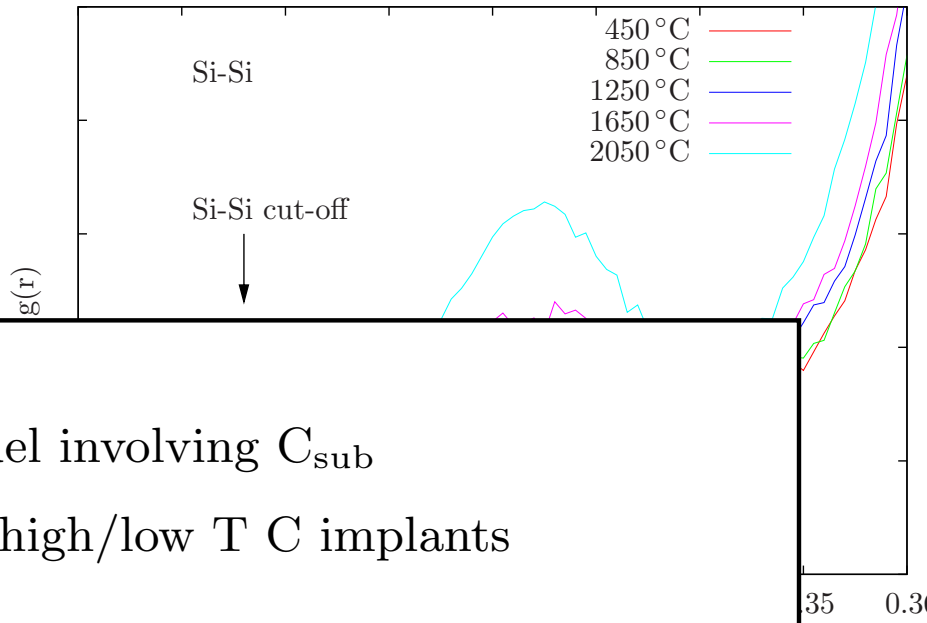

Stretched SiC in c-Si

- Consistent to precipitation model involving C_{sub}
- Explains annealing behavior of high/low T C implants
  - Low T: highly mobiel C_i
  - High T: stable configurations of C_{sub}

$\Rightarrow$ High T $\leftrightarrow$ IBS conditions far from equilibrium

$\Rightarrow$ Precipitation mechanism involving C_{sub}

°C)

Si-Si bonds: Si-C_{sub}-Si along $\langle 1\,1\,0 \rangle$ ($\rightarrow$ 0.325 nm)

C-C bonds:

- C-C next neighbour pairs reduced (mandatory)
- Peak at 0.3 nm slightly shifted
  - C-Si $\langle 1\,0\,0 \rangle$ combinations (dashed arrows)
    $\rightarrow$ C-Si $\langle 1\,0\,0 \rangle$ & C_{sub} combinations (|)
    $\rightarrow$ pure C_{sub} combinations (↓)
  - Range [|-↓]: C_{sub} & C_{sub} with nearby Si_I

Increased temperature simulations at high C concentration

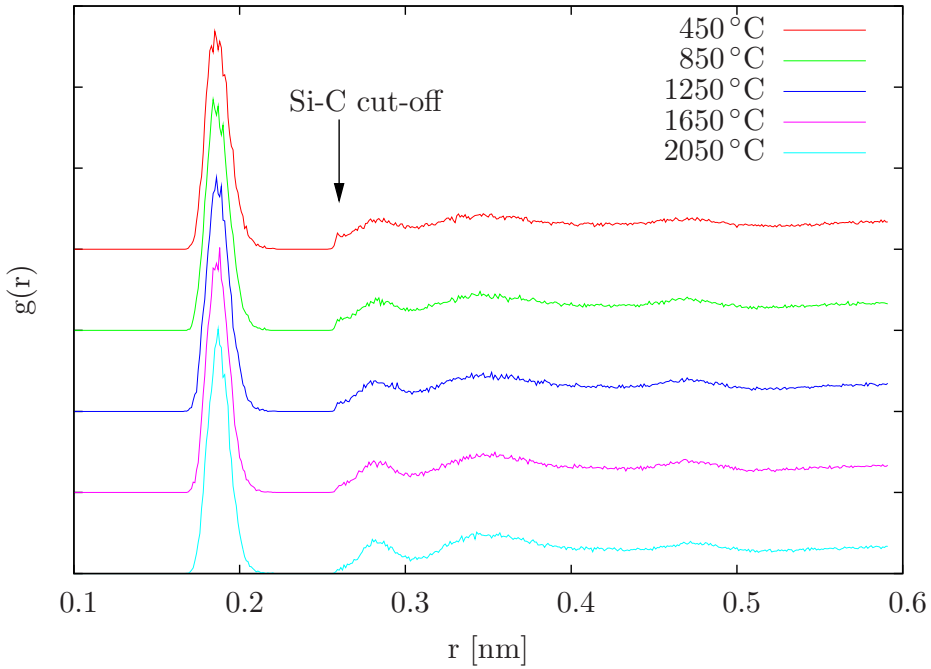

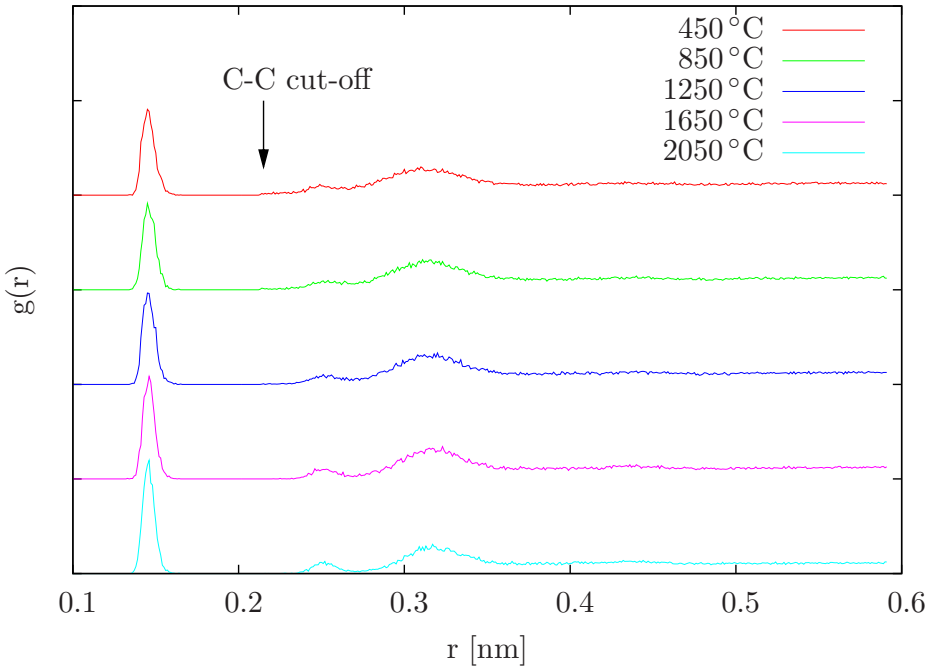

0.186 nm: Si-C pairs ↑
(as expected in 3C-SiC)

0.282 nm: Si-C-C

≈0.35 nm: C-Si-Si

0.15 nm: C-C pairs ↑
(as expected in graphite/diamond)

0.252 nm: C-C-C (2^{nd} NN for diamond)

0.31 nm: shifted towards 0.317 nm → C-Si-C

- Decreasing cut-off artifact
- Amorphous SiC-like phase remains
- High amount of damage & alignement to c-Si host matrix lost
- Slightly sharper peaks ⇒ indicate slight acceleration of dynamics due to temperature

High C & small V & short t ⇒ Slow restructuring due to strong C-C bonds ⇐ High C & low T implants

Summary and Conclusions

Pecipitation simulations

- High C concentration → amorphous SiC like phase
- Problem of potential enhanced slow phase space propagation
- Low T → C-Si ⟨1 0 0⟩ dumbbell dominated structure
- High T → C_{sub} dominated structure
- High T necessary to simulate IBS conditions (far from equilibrium)
- Precipitation by successive agglomeration of C_{sub}(epitaxy)
- Si_i: vehicle to form C_{sub} & supply of Si & stress compensation (stretched SiC, interface)

Defects

- DFT / EA
  - Point defects excellently / fairly well described by DFT / EA
  - C_{sub} drastically underestimated by EA
  - EA predicts correct ground state: C_{sub} & Si_i > C_i
  - Identified migration path explaining diffusion and reorientation experiments by DFT
  - EA fails to describe C_i migration: Wrong path & overestimated barrier
- Combinations of defects
  - Agglomeration of point defects energetically favorable by compensation of stress
  - Formation of C-C unlikely
  - C_{sub} favored conditions (conceivable in IBS)
  - C_i ⟨1 0 0⟩ ↔ C_{sub} & Si_i ⟨1 1 0⟩
    Low barrier (0.77 eV) & low capture radius

Precipitation by successive agglomeration of C_{sub}

Acknowledgements

Thanks to ...

Augsburg

- Prof. B. Stritzker (accomodation at EP IV)
- Ralf Utermann (EDV)

Helsinki

- Prof. K. Nordlund (MD)

Munich

- Bayerische Forschungsstiftung (financial support)

Paderborn

- Prof. J. Lindner (SiC)
- Prof. G. Schmidt (DFT + financial support)
- Dr. E. Rauls (DFT + SiC)
- Dr. S. Sanna (VASP)

Thank you for your attention!